INF-SUP STABILIZED SCOTT–VOGELIUS PAIRS ON GENERAL SIMPLICIAL GRIDS BY RAVIART–THOMAS ENRICHMENT

VOLKER JOHN, XU LI, CHRISTIAN MERDON, AND HONGXING RUI

Abstract. This paper considers the discretization of the Stokes equations with Scott–Vogelius pairs of finite element spaces on arbitrary shape-regular simplicial grids. A novel way of stabilizing these pairs with respect to the discrete inf-sup condition is proposed and analyzed. The key idea consists in enriching the continuous polynomials of order k of the Scott–Vogelius velocity space with appropriately chosen and explicitly given Raviart–Thomas bubbles. This approach is inspired by [Li/Rui, IMA J. Numer. Anal, 2021], where the case $k = 1$ was studied. The proposed method is pressure-robust, with optimally converging $\boldsymbol{H}^1$-conforming velocity and a small $\boldsymbol{H}(\mathrm{div})$-conforming correction rendering the full velocity divergence-free. For $k \geqslant d$, with d being the dimension, the method is parameter-free. Furthermore, it is shown that the additional degrees of freedom for the Raviart–Thomas enrichment and also all non-constant pressure degrees of freedom can be condensated, effectively leading to a pressure-robust, inf-sup stable, optimally convergent $\boldsymbol{P}_k \times P_0$ scheme. Aspects of the implementation are discussed and numerical studies confirm the analytic results.

1. Introduction

The research on divergence-free schemes for incompressible flow equations is a very active field of research as these schemes have desirable properties with respect to mass conservation and other structure preservation features. A very important feature is pressure-robustness [31, 25], which guarantees that the balancing of gradient forces by the pressure gradient is correctly transferred from the continuous problem to the discrete problem, such that the discrete velocity is zero whenever the right-hand side force is a gradient. The same holds for the balancing of the irrotational part of the material derivative in time-dependent Navier–Stokes flows [17]. It was shown that non-pressure-robust schemes can lead to discrete velocity solutions that have errors which scale with the inverse viscosity [30, 25], or even to suboptimal convergence rates in time-dependent Stokes problems [32]. Also optimal estimates for more complicated flow problems seem to benefit from pressure-robustness [35, 34, 1, 5, 23, 16].

It should be also noted that the set of divergence-free schemes and the set of pressure-robust schemes are not subsets of each other, as there are non-divergence-free schemes that can be made pressure-robust by a reconstruction operator technique [31, 26]. On the other hand, there are divergence-free methods that are not necessarily pressure-robust, like virtual element methods without a proper right-hand side discretization, see [15, 12]. In practice, many non-divergence-free schemes are used together with grad-div stabilization. This technique reduces or even removes the explicit dependence of the constants in error bounds on

Date: 6th June 2022.

2020 *Mathematics Subject Classification.* 65N12, 65N30, 76D07.

Key words and phrases. Finite element methods, Stokes equations, divergence-free, pressure-robustness.

The second author was supported by the China Scholarship Council (No. 202106220106) and the National Natural Science Foundation of China (No. 12131014). The third author gratefully acknowledges the funding by the German Science Foundation (DFG) within the project "ME 4819/2-1". The fourth author was supported by the National Natural Science Foundation of China (No. 12131014).

inverse powers of the viscosity, e.g., see [14] for the evolutionary Navier–Stokes equations. However, it possesses also certain drawbacks, as it introduces a user-chosen parameter and it is not mass-conservative.

This paper focuses on divergence-free inf-sup stable schemes, where the notion 'divergence-free' will be always used in the sense of 'weakly divergence-free', i.e., the divergence is zero in the sense of $L^2(\Omega)$. To this end, the stationary Stokes equations in a bounded domain $\Omega \subset \mathbb{R}^d$, $d \in \{2,3\}$, are considered

$$\begin{aligned} -\nu\Delta \boldsymbol{u} + \nabla p &= \boldsymbol{f} && \text{in } \Omega, \\ \operatorname{div}(\boldsymbol{u}) &= 0 && \text{in } \Omega, \\ \boldsymbol{u} &= \boldsymbol{0} && \text{on } \partial\Omega. \end{aligned} \tag{1.1}$$

The boundary $\partial\Omega$ of Ω is assumed to be polyhedral and Lipschitz continuous. Problem (1.1) is already written in a dimensionless form, where the kinematic viscosity $\nu \in \mathbb{R}$ with $\nu > 0$ and the forces $\boldsymbol{f}$ are the given data. The unknown functions are the velocity field $\boldsymbol{u}$ and the pressure p. System (1.1) is transferred in the usual way to a weak formulation, which reads: Find $(\boldsymbol{u}, p) \in \boldsymbol{V} \times Q := \boldsymbol{H}_0^1(\Omega) \times L_0^2(\Omega)$ such that

$$\begin{aligned} (\nu\nabla \boldsymbol{u}, \nabla \boldsymbol{v}) - (\operatorname{div}(\boldsymbol{v}), p) &= (\boldsymbol{f}, \boldsymbol{v}) && \forall\, \boldsymbol{v} \in \boldsymbol{V}, \\ (\operatorname{div}(\boldsymbol{u}), q) &= 0 && \forall\, q \in Q. \end{aligned} \tag{1.2}$$

Here, $\boldsymbol{H}_0^1(\Omega)$ is the vector-valued Sobolev space of functions where each component is in $H^1(\Omega)$ and has a vanishing trace on $\partial\Omega$, $L_0^2(\Omega)$ is the space of functions from $L^2(\Omega)$ with vanishing integral mean value, $(\cdot,\cdot)$ denotes the inner product in $L^2(\Omega)$ and $\boldsymbol{L}^2(\Omega)$, and it is assumed that $\boldsymbol{f} \in \boldsymbol{L}^2(\Omega)$. By the theory of linear saddle point problems, using the so-called inf-sup condition, it is known that (1.2) possesses a unique solution, e.g., see [18, 24].

Since the inf-sup stability is a necessary condition for the well-posedness of a linear saddle point problem, the construction of classical Galerkin finite element schemes traditionally focused on the satisfaction of a discrete counterpart of this condition. Let $\boldsymbol{V}_h$ and Q_h denote finite element velocity and pressure spaces, respectively, then the Galerkin method seeks $(\boldsymbol{u}_h, p_h) \in \boldsymbol{V}_h \times Q_h$ such that

$$\begin{aligned} (\nu\nabla \boldsymbol{u}_h, \nabla \boldsymbol{v}_h) - (\operatorname{div}(\boldsymbol{v}_h), p_h) &= (\boldsymbol{f}, \boldsymbol{v}_h) && \forall\, \boldsymbol{v}_h \in \boldsymbol{V}_h, \\ (\operatorname{div}(\boldsymbol{u}_h), q_h) &= 0 && \forall\, q_h \in Q_h. \end{aligned} \tag{1.3}$$

It turned out that the goal of satisfying a discrete inf-sup condition was often achieved only by relaxing the divergence constraint, i.e., the mass conservation is, often by far, not satisfied exactly, e.g., see [25]. Given a finite element velocity space $\boldsymbol{V}_h$, then the properties of inf-sup stability and mass conservation lead in fact to different requirements: for the satisfaction of the discrete inf-sup condition, Q_h should be sufficiently small and for the exact satisfaction of the divergence constraint, Q_h should be sufficiently large, compare [24, Rem. 3.56].

The starting point of the method proposed and analyzed in the current paper is the pair of spaces $\boldsymbol{V}_h \times Q_h = \boldsymbol{P}_k \times P_{k-1}^{\text{disc}}$, $k \geqslant 1$, on simplicial triangulations, where $\boldsymbol{P}_k$ is the space of continuous and piecewise polynomial vector-valued functions with polynomial degree k and P_{k-1}^{disc} is the space of piecewise polynomial functions with polynomial degree $k-1$. As usual, the notation does not contain the facts that $\boldsymbol{P}_k$ is intersected with $\boldsymbol{V}$ and P_{k-1}^{disc} with Q. For $k \geqslant d$, this pair of spaces is also known as Scott–Vogelius pair [36, 37, 4, 41, 33]. It is $\operatorname{div}(\boldsymbol{P}_k) \subseteq P_{k-1}^{\text{disc}}$, so that if $\boldsymbol{u}_h$ is a velocity solution of (1.3), one can choose $q_h = \operatorname{div}(\boldsymbol{u}_h)$ in the discrete divergence constraint, leading to

$$(\operatorname{div}(\boldsymbol{u}_h), \operatorname{div}(\boldsymbol{u}_h)) = \|\operatorname{div}(\boldsymbol{u}_h)\|^2 = 0, \tag{1.4}$$

which means that $\boldsymbol{u}_h$ is divergence-free. This property is our major motivation for studying Scott–Vogelius pairs. However, it is well known that the discrete inf-sup condition for these pairs is valid only for certain classes of meshes and if k is sufficiently large, e.g., see [42, 21, 22]. In particular, for $d = 3$, which is the interesting case in applications, the smallest value is $k = 3$ for so-called barycentric-refined meshes [41]. For $k = 2$ there is a related method on Powell-Sabin tetrahedral grids with an implicitly defined pressure subspace [43].

This paper addresses the cases where the inf-sup stability is not given. For such cases, an enrichment of the discrete velocity space is proposed that consists of local functions, locally very few, which leads to discrete velocity fields that satisfy (1.4) and to pressure-robust velocity error estimates. The last two properties are in contrast to previous proposals, like the family of Bernardi–Raugel elements that add higher-order polynomial bubbles [6]. Moreover, the proposed method is easy to implement, in particular it does not involve any face integrals.

In the literature there are meanwhile several approaches for constructing divergence-free pairs of finite element spaces. In [19, 20, 10], $\boldsymbol{H}^1$-conforming functions are utilized for enriching the velocity space, which are however non-standard and not available in many finite element codes. Another strategy employs the Stokes complex of lowest regularity where the velocity is searched only in $\boldsymbol{H}(\mathrm{div})$, e.g., see [11, 38, 2]. This approach leads to the nowadays quite popular hybrid discontinuous Galerkin methods (HDG) [9, 28].

In this paper we propose and analyze an approach for enriching Scott–Vogelius pairs by $\boldsymbol{H}(\mathrm{div})$-conforming functions. The main idea of the method is inspired by [29], where the lowest-order case $k = 1$ is studied. Therein a novel scheme was suggested which preserves the features of the $\boldsymbol{H}^1$-conforming formulation while using a simple lowest-order Raviart–Thomas enrichment. It turns out that there are for $k \geqslant 2$ new aspects in the construction of the method and additional difficulties in their numerical analysis. The standard polynomial space $\boldsymbol{P}_k$ is enriched with an $\boldsymbol{H}(\mathrm{div})$-conforming subspace of specially chosen but standard Raviart–Thomas functions, which ensures that the discrete inf-sup condition holds and that the divergence constraint is satisfied exactly on general unstructured shape-regular simplicial meshes. In particular no assumption on non-singular vertices is needed. The added $\boldsymbol{H}(\mathrm{div})$-conforming part vanishes in the limit $h \to 0$, while the $\boldsymbol{H}^1$-conforming part is an approximation of the velocity of optimal order. If $k < d$, the lowest-order Raviart–Thomas space is involved, while for the higher order cases $k \geqslant d$, only interior non-divergence-free Raviart–Thomas bubbles of order $k - 1$ are used for the enrichment. These additional degrees of freedom ensure the inf-sup stability of the scheme and lead to a pressure-robust $\boldsymbol{H}^1$-conforming solution, which can be turned into a divergence-free solution by adding the $\boldsymbol{H}(\mathrm{div})$-conforming Raviart–Thomas correction.

A subtle point of the proposed method is that the space $\boldsymbol{P}_k$, $k \geqslant 2$, and the enrichment space might have a non-zero intersection on certain triangulations, for which we also provide an example. Nevertheless, it is ensured that the method selects a unique discrete solution. For $k < d$ there is a stabilization on the lowest-order Raviart–Thomas part, which involves a parameter and essentially penalizes this part of the enrichment component, as in the original scheme for $k = 1$ from [29]. For any higher-order Raviart–Thomas part, no stabilization is needed, hence the scheme is parameter-free for $k \geqslant d$, and the uniqueness follows instead from the bijectivity of the divergence operator with respect to the enrichment space and the divergence constraint.

The final result of the paper concerns a condensed method in the spirit of other divergence-free schemes [27, 13, 39]. Indeed, it is possible to statically condensate the additional Raviart–Thomas velocity degrees of freedom and the higher order pressure degrees of freedom, effectively resulting in a $\boldsymbol{P}_k \times P_0$ scheme. The condensed scheme preserves all the properties of the full scheme and the missing degrees of freedom can be restored by a cheap post-processing. Behind this transformation of the problem is a correction operator that maps each conforming polynomial test function to a Raviart–Thomas correction such that the divergence of their sum is a piecewise constant.

The paper is structured as follows. Section 2 explains the main concept of the scheme and explicitly constructs the needed Raviart–Thomas subspaces for enrichment up to a certain order. The full discrete problem is presented in Section 3 and the mechanisms behind the uniqueness of the solution are discussed. In Section 4 it is shown that the enrichment spaces ensure inf-sup stability, i.e., the missing ingredient for unique solvability. Section 5 derives optimal a priori error estimates for the velocity and the pressure via standard arguments. The derivation of the condensed scheme and the post-processing technique for recovering the full solution are presented in Section 6. Some numerical studies in Section 7 confirm the results in two and three dimensions and for different polynomial orders k. The paper closes with a summary and outlook.

2. Main concept

This section explains the main concept and the design of the Raviart–Thomas enrichment spaces used in the suggested method.

2.1. **Notation and preliminaries.** Consider a regular triangulation $\mathcal{T}$ of the domain Ω with nodes $\mathcal{N}$ and facets $\mathcal{F}$. The set of all interior faces is denoted by $\mathcal{F}^0$. Denote by h_T the diameter of elements $T \in \mathcal{T}$ and define $h := \max_{T\in\mathcal{T}} h_T$ as well as the piecewise constant function $h_{\mathcal{T}}$ via $h_{\mathcal{T}}|_T := h_T$ for all $T \in \mathcal{T}$.

The space of scalar-valued polynomials of order k on a subdomain ω is denoted by $P_k(\omega)$ and is written in bold for vector-valued polynomial spaces. The subspace of divergence-free functions is denoted by

$$\boldsymbol{V}_0 := \{\boldsymbol{v} \in \boldsymbol{V} : \operatorname{div}(\boldsymbol{v}) = 0\}.$$

Also define

$$P_k(\mathcal{T}) := \left\{q_h \in H^1(\Omega) : q_h|_T \in P_k(T) \text{ for all } T \in \mathcal{T}\right\},$$

and

$$P_k^{\text{disc}}(\mathcal{T}) := \left\{q_h \in L^2(\Omega) : q_h|_T \in P_k(T) \text{ for all } T \in \mathcal{T}\right\}.$$

Furthermore, the space of Raviart–Thomas functions on a cell $T \in \mathcal{T}$ is given by

$$\boldsymbol{RT}_k(T) := \left\{\boldsymbol{v} \in \boldsymbol{L}^2(T) : \exists \boldsymbol{p} \in \boldsymbol{P}_k(T), q \in P_k(T),\ \boldsymbol{v}|_T(\boldsymbol{x}) = \boldsymbol{p}(\boldsymbol{x}) + q(\boldsymbol{x})\boldsymbol{x}\right\}$$

and it is the building block of the global space

$$\boldsymbol{RT}_k(\mathcal{T}) := \{\boldsymbol{v} \in \boldsymbol{H}(\operatorname{div}, \Omega) : \forall T \in \mathcal{T}\ \boldsymbol{v}|_T \in \boldsymbol{RT}_k(T)\}.$$

The Raviart–Thomas subspace of interior bubble functions reads

$$\boldsymbol{RT}_k^{\text{int}}(\mathcal{T}) := \{\boldsymbol{v} \in \boldsymbol{RT}_k(\mathcal{T}) : \boldsymbol{v} \cdot \boldsymbol{n}_T|_{\partial T} = 0 \text{ for all } T \in \mathcal{T}\},$$

where $\boldsymbol{n}_T$ is the outer unit normal vector along ∂T. The subspace of $\boldsymbol{RT}_k^{\text{int}}(\mathcal{T})$ consisting of divergence-free functions and its arbitrary but fixed complement space are denoted by $\boldsymbol{RT}_{k,0}^{\text{int}}(\mathcal{T})$ and $\widetilde{\boldsymbol{RT}}_k^{\text{int}}(\mathcal{T})$, respectively, i.e.,

$$\boldsymbol{RT}_k^{\text{int}}(\mathcal{T}) = \boldsymbol{RT}_{k,0}^{\text{int}}(\mathcal{T}) \oplus \widetilde{\boldsymbol{RT}}_k^{\text{int}}(\mathcal{T}).$$

The only divergence-free function in $\widetilde{\boldsymbol{RT}}_k^{\text{int}}(\mathcal{T})$ is the zero function, which implies that the divergence operator on this space is injective. Note that $\widetilde{\boldsymbol{RT}}_k^{\text{int}}(\mathcal{T})$ is not unique in general cases. Here we require that its local spaces $\widetilde{\boldsymbol{RT}}_k^{\text{int}}(T), T \in \mathcal{T}$, have the same structure in the sense that all of them are connected to a same reference space via Piola's transformation (see e.g. [7, Eq. 2.1.69]). This is natural for $\widetilde{\boldsymbol{RT}}_k^{\text{int}}(\mathcal{T})$ since it is characterized by the normal trace and the divergence, which are preserved (in a scaled meaning) by Piola's transformation.

The subspace of $P_k^{\text{disc}}(\mathcal{T})$ consisting of elementwise zero-mean functions is defined as

$$\widetilde{P}_k^{\text{disc}}(\mathcal{T}) := \left\{ q_h \in P_k^{\text{disc}}(\mathcal{T}) : (q_h, 1)_T = 0 \text{ for all } T \in \mathcal{T} \right\}. \tag{2.1}$$

Note that $\boldsymbol{RT}_0^{\text{int}}(\mathcal{T}) = \widetilde{\boldsymbol{RT}}_0^{\text{int}}(\mathcal{T}) = \{\mathbf{0}\}$ and $\widetilde{P}_0^{\text{disc}}(\mathcal{T}) = \{0\}$.

Throughout this paper, for any (scalar or vector-valued) finite element space $\mathcal{S}$ (with or without an argument like $\mathcal{T}$), its local version on each element T is denoted by $\mathcal{S}(T)$ if not specially indicated. The symbol $\pi_{\mathcal{S}}$ ($\pi_{\mathcal{S}(T)}$) is used to denote the L^2 projection operator onto $\mathcal{S}$ ($\mathcal{S}(T)$, respectively).

2.2. **Enrichment approach.** For a given $k \geqslant 1$, we define the $\boldsymbol{H}^1$-conforming velocity ansatz space of piecewise vector-valued polynomials

$$\boldsymbol{V}_h^{\text{ct}} := \boldsymbol{P}_k(\mathcal{T}) \cap \boldsymbol{V}$$

and the desired pressure space

$$Q_h := P_{k-1}^{\text{disc}}(\mathcal{T}) \cap Q.$$

In general, without further assumptions on the mesh or k, one has to expect a violation of the inf-sup stability. However, we can always assume the existence of a sufficiently small auxiliary piecewise pressure subspace $\widehat{Q}_h = (\bigcup_{T\in\mathcal{T}} \widehat{Q}_h(T)) \cap Q$ with $\widehat{Q}_h(T) \subseteq P_{k-1}(T)$ (it can be sometimes only the zero space) such that $(\boldsymbol{V}_h^{\text{ct}}, \widehat{Q}_h)$ is inf-sup stable. Consider now the L^2 orthogonal split of Q_h into $Q_h = \widehat{Q}_h \oplus_{L^2} \widehat{Q}_h^{\perp}$. The main motivation for finding the enrichment space $\boldsymbol{V}_h^{\text{R}}$ is twofold: on the one hand, $\boldsymbol{V}_h^{\text{R}}$ should fix the potential spurious pressure modes in $\widehat{Q}_h^{\perp}$; on the other hand, $\operatorname{div}(\boldsymbol{V}_h^{\text{R}}) \subseteq Q_h$ guarantees that the discrete velocity is still divergence-free.

In fact, we suggest to select a subspace of $\boldsymbol{RT}_{k-1}$ such that either

$$\operatorname{div} : \boldsymbol{V}_h^{\text{R}} \to \widehat{Q}_h^{\perp} \quad \text{is bijective for } k \geqslant d, \tag{2.2}$$

or

$$\operatorname{div} : \boldsymbol{V}_h^{\text{R}} \to \widehat{Q}_h^{\perp} \quad \text{is surjective for } k < d. \tag{2.3}$$

Eventually, it is shown that an inf-sup stable scheme for the velocity space $\boldsymbol{V}_h := \boldsymbol{V}_h^{\text{ct}} \times \boldsymbol{V}_h^{\text{R}}$ and the full pressure space Q_h can be established, such that its solution $\boldsymbol{u}_h = (\boldsymbol{u}_h^{\text{ct}}, \boldsymbol{u}_h^{\text{R}}) \in \boldsymbol{V}_h^{\text{ct}} \times \boldsymbol{V}_h^{\text{R}}$ is divergence-free in the sense that $\operatorname{div}(\boldsymbol{u}_h^{\text{ct}} + \boldsymbol{u}_h^{\text{R}}) = 0$.

Table 2.1. Enrichment spaces for $d = 2$ and $k = 1, 2, 3, 4$.

k	$\widehat{Q}_h(T)$	$\dim(\widehat{Q}_h^{\perp}(T))$	$\dim(\boldsymbol{V}_h^{\mathrm{R}}(T))$	
1	$\{0\}$	1	3	full $\boldsymbol{RT}_0(T)$
2	$P_0(T)$	2	2	full $\boldsymbol{RT}_1^{\mathrm{int}}(T)$
3	$P_1(T)$	3	3	from $\widetilde{\boldsymbol{RT}}_2^{\mathrm{int}}(T)$
4	$P_2(T)$	4	4	from $\widetilde{\boldsymbol{RT}}_3^{\mathrm{int}}(T)$

Table 2.2. Enrichment spaces for $d = 3$ and $k = 1, 2, 3$.

k	$\widehat{Q}_h(T)$	$\dim(\widehat{Q}_h^{\perp}(T))$	$\dim(\boldsymbol{V}_h^{\mathrm{R}}(T))$	
1	$\{0\}$	1	4	full $\boldsymbol{RT}_0(T)$
2	$\{0\}$	4	7	full $\boldsymbol{RT}_0(T)$ & full $\boldsymbol{RT}_1^{\mathrm{int}}(T)$
3	$P_0(T)$	9	9	from $\widetilde{\boldsymbol{RT}}_2^{\mathrm{int}}(T)$

Of course, the choice of $\widehat{Q}_h$ is not unique in general. Properties (2.2) and (2.3) are the fundamental principles for selecting the spaces. Tables 2.1 and 2.2 list some guaranteed inf-sup stable pairs $(\boldsymbol{V}_h^{\mathrm{ct}}, \widehat{Q}_h)$, implied, e.g., by [7, Sec. 8.6-8.7], for different k in two and three dimensions, respectively. The other columns in these tables state the expected dimension of the enrichment spaces and some hint on how the enrichment functions can be chosen in each case. Their detailed construction is explained in the next subsection where it is also shown that the divergence operator between $\boldsymbol{V}_h^{\mathrm{R}}$ and $\widehat{Q}_h^{\perp}$ is bijective (except for $k < d$). Generalizing the examples from Tables 2.1 and 2.2, the space $\widehat{Q}_h$ can be chosen as

$$\widehat{Q}_h := \begin{cases} \{\mathbf{0}\} & k < d, \\ P_{k-d}^{\mathrm{disc}}(\mathcal{T}) \cap Q & k \geqslant d, \end{cases} \tag{2.4}$$

and the corresponding Raviart–Thomas enrichment space $\boldsymbol{V}_h^{\mathrm{R}}$ is chosen as

$$\boldsymbol{V}_h^{\mathrm{R}} := \begin{cases} \boldsymbol{RT}_0(\mathcal{T}) \cap \boldsymbol{H}_0(\mathrm{div}, \Omega) & k = 1, \\ (\boldsymbol{RT}_0(\mathcal{T}) \cap \boldsymbol{H}_0(\mathrm{div}, \Omega)) \oplus \boldsymbol{RT}_1^{\mathrm{int}}(\mathcal{T}) & k = 2, d = 3, \\ \left\{ \boldsymbol{v}_h \in \widetilde{\boldsymbol{RT}}_{k-1}^{\mathrm{int}}(\mathcal{T}) : \mathrm{div}(\boldsymbol{v}_h) \in \widehat{Q}_h^{\perp} \right\} & k \geqslant d. \end{cases} \tag{2.5}$$

Here, $\boldsymbol{H}_0(\mathrm{div}, \Omega)$ denotes the space of functions from $\boldsymbol{H}(\mathrm{div}, \Omega)$ with zero normal trace along $\partial\Omega$. The local dimension of $\boldsymbol{V}_h^{\mathrm{R}}$ is

$$\dim\left(\boldsymbol{V}_h^{\mathrm{R}}(T)\right) = \begin{cases} d+1 & k = 1, \\ \dim\left(P_{k-1}(T)\right) - \dim\left(P_{k-2}(T)\right) = k & k \geqslant 2, d = 2, \\ 7 & k = 2, d = 3, \\ \dim\left(P_{k-1}(T)\right) - \dim\left(P_{k-3}(T)\right) = k^2 & k \geqslant 3, d = 3. \end{cases}$$

Throughout this paper, the analysis for $k < d$ cases is based on the spaces by (2.5), while for $k \geqslant d$ cases we only require $\widehat{Q}_h(T) \supseteq P_0(T)$ and further $\boldsymbol{V}_h^{\mathrm{R}} \times \widehat{Q}_h^{\perp} \subseteq \widetilde{\boldsymbol{RT}}_{k-1}^{\mathrm{int}}(\mathcal{T}) \times \widetilde{P}_{k-1}^{\mathrm{disc}}(\mathcal{T})$ satisfies (2.2). Indeed, from the separation of $\boldsymbol{H}(\mathrm{div})$-conforming finite element spaces, e.g., as in [27, § 2.2.4] and [40, § 5.2-5.3], one can verify that $\mathrm{div} : \boldsymbol{RT}_k^{\mathrm{int}}(\mathcal{T}) \to \widetilde{P}_k^{\mathrm{disc}}(\mathcal{T})$ is a surjective operator and thus $\mathrm{div} : \widetilde{\boldsymbol{RT}}_k^{\mathrm{int}}(\mathcal{T}) \to \widetilde{P}_k^{\mathrm{disc}}(\mathcal{T})$ is a bijective operator. Also note that $\widetilde{\boldsymbol{RT}}_1^{\mathrm{int}}(\mathcal{T}) = \boldsymbol{RT}_1^{\mathrm{int}}(\mathcal{T})$.

Remark 2.1 (On over-enrichment)**.** There may be cases where a larger space $\widehat{Q}_h$ and hence a smaller enrichment space is sufficient. This is certainly also connected to the mesh properties. To give one example: if the mesh is a barycentric refinement of some given mesh, then inf-sup stability is already ensured for the full pressure space, i.e., $\widehat{Q}_h = Q_h$ for $k \geqslant d$ is a valid choice, which results in the Scott–Vogelius finite element family [36, 4, 41]. Also in case of unstructured grids with non-singular vertices, positive results for $k \geqslant 3$ in two dimensions are known [21, 22]. From this perspective our schemes can be seen as a stabilization of the Scott–Vogelius family that ensures inf-sup stability on general shape-regular meshes, even with singular vertices, that works for any $k \geqslant 1$.

Moreover, it turns out that a potential over-enrichment is not really an issue in practice. In fact, Section 6 explains how all additional enrichment degrees of freedom can be effectively condensated. By 'over-enrichment', the pressure space can be even decreased to piecewise constants without compromising any qualitative properties of the scheme.

2.3. **Explicit constructions of the enrichment space.** This subsection discusses explicit element-wise constructions of basis functions of $\boldsymbol{V}_h^{\mathrm{R}}$ for $k = 2, \dots, 6-d$ beyond the $k = 1$ case in [29]. To fix local enumerations, consider a simplex $T \in \mathcal{T}$ with faces F_j and their respective opposing vertex $\boldsymbol{P}_j$ with nodal basis function φ_j. The lowest-order Raviart–Thomas functions read

$$\boldsymbol{\psi}_j^{\mathrm{RT}_0} := \frac{1}{d|T|}\left(\boldsymbol{x} - \boldsymbol{P}_j\right) \quad \text{such that} \quad \int_{F_k} \boldsymbol{\psi}_j^{\mathrm{RT}_0} \cdot \boldsymbol{n}_T \, ds = \delta_{jk},$$

for $j, k = 1, \dots, d+1$. By a multiplication of these basis functions with their opposite nodal basis functions, one obtains the interior Raviart–Thomas functions

$$\boldsymbol{\psi}_j^{\mathrm{RT}_1} := \varphi_j \boldsymbol{\psi}_j^{\mathrm{RT}_0} \in \widetilde{\boldsymbol{RT}}_1^{\mathrm{int}}(T).$$

Note that only d of them are linearly independent. Indeed it holds $\boldsymbol{\psi}_{d+1}^{\mathrm{RT}_1} = -\sum_{j=1}^{d} \boldsymbol{\psi}_j^{\mathrm{RT}_1}$.

Lemma 2.2 (Explicit design of $\boldsymbol{V}_h^{\mathrm{R}}$ for $d = 2$)**.** On any $T \in \mathcal{T}$, the following statements hold:

(a) The functions $\{\boldsymbol{\psi}_j^{\mathrm{RT}_1}\}_{j=1,2} \subset \widetilde{\boldsymbol{RT}}_1^{\mathrm{int}}(T)$ are linearly independent and it holds

$$\int_T \operatorname{div}(\boldsymbol{\psi}_j^{\mathrm{RT}_1}) \, d\boldsymbol{x} = 0.$$

For $\boldsymbol{V}_h^{\mathrm{R}}(T) := \operatorname{span}\{\boldsymbol{\psi}_1^{\mathrm{RT}_1}, \boldsymbol{\psi}_2^{\mathrm{RT}_1}\} = \widetilde{\boldsymbol{RT}}_1^{\mathrm{int}}(T)$ the restricted divergence operator

$$\operatorname{div} : \boldsymbol{V}_h^{\mathrm{R}}(T) \to \widehat{Q}_h^{\perp}(T) \quad \text{for } \widehat{Q}_h(T) = P_0(T) \quad \text{is bijective.}$$

(b) The functions

$$\boldsymbol{\psi}_j^{\mathrm{RT}_2} := \left(5\varphi_j - 2\right) \boldsymbol{\psi}_j^{\mathrm{RT}_1} \in \widetilde{\boldsymbol{RT}}_2^{\mathrm{int}}(T) \quad \text{for } j = 1, 2, 3,$$

are linearly independent and it holds

$$\int_T \operatorname{div}(\boldsymbol{\psi}_j^{\mathrm{RT}_2}) \varphi_k \, d\boldsymbol{x} = 0 \quad \text{for } j, k = 1, 2, 3.$$

For $\boldsymbol{V}_h^{\mathrm{R}}(T) := \operatorname{span}\{\boldsymbol{\psi}_j^{\mathrm{RT}_2} : j = 1, 2, 3\}$ the restricted divergence operator

$$\operatorname{div} : \boldsymbol{V}_h^{\mathrm{R}}(T) \to \widehat{Q}_h^{\perp}(T) \quad \text{for } \widehat{Q}_h(T) = P_1(T) \quad \text{is bijective.}$$

(c) The three auxiliary face-related functions

$$\boldsymbol{\psi}_j^{\mathrm{RT}_3} := \frac{1}{7}\left(7\varphi_j^2 - 6\varphi_j + 1\right)\boldsymbol{\psi}_j^{\mathrm{RT}_1} \in \widetilde{\boldsymbol{RT}}_3^{\mathrm{int}}(T) \quad \text{for } j = 1,2,3,$$

and additionally

$$\boldsymbol{\psi}_4^{\mathrm{RT}_3} := -2\varphi_2\varphi_3\boldsymbol{\psi}_2^{\mathrm{RT}_1} + \frac{2}{45}\left(\boldsymbol{\psi}_1^{\mathrm{RT}_1} + 5\boldsymbol{\psi}_2^{\mathrm{RT}_1}\right) + \frac{1}{70}\left(3\boldsymbol{\psi}_1^{\mathrm{RT}_2} + 2\boldsymbol{\psi}_2^{\mathrm{RT}_2} - 3\boldsymbol{\psi}_3^{\mathrm{RT}_2}\right) \in \widetilde{\boldsymbol{RT}}_3^{\mathrm{int}}(T),$$

are linearly independent and it holds

$$\int_T \mathrm{div}(\boldsymbol{\psi}_j^{\mathrm{RT}_3})\lambda_h \, d\boldsymbol{x} = 0 \quad \text{for } \lambda_h \in P_2(T), j = 1,2,3,4.$$

For $\boldsymbol{V}_h^{\mathrm{R}}(T) := \mathrm{span}\{\boldsymbol{\psi}_j^{\mathrm{RT}_3} : j = 1,2,3,4\}$ the restricted divergence operator

$$\mathrm{div} : \boldsymbol{V}_h^{\mathrm{R}}(T) \to \widehat{Q}_h^{\perp}(T) \quad \text{for } \widehat{Q}_h(T) = P_2(T) \quad \text{is bijective.}$$

Proof of (a). By simple calculations on the reference element and a dimension argument, one can obtain

$$\int_T \mathrm{div}(\boldsymbol{\psi}_j^{\mathrm{RT}_1})\varphi_k \, d\boldsymbol{x} = \frac{3\delta_{jk} - 1}{24} \quad \text{for } j,k = 1,2,3. \tag{2.6}$$

Then the linear independence of $\boldsymbol{\psi}_1^{\mathrm{RT}_1}$ and $\boldsymbol{\psi}_2^{\mathrm{RT}_1}$ follows from $\det(A) = \frac{1}{192} \neq 0$ with $A = (a_{jk}) := (\int_T \mathrm{div}(\boldsymbol{\psi}_j^{\mathrm{RT}_1})\varphi_k \, d\boldsymbol{x}) \in \mathbb{R}^{2\times 2}$. In fact, if there exists a vector $\vec{c} = (c_1, c_2) \in \mathbb{R}^2$ which makes $c_1\mathrm{div}(\boldsymbol{\psi}_1^{\mathrm{RT}_1}) + c_2\mathrm{div}(\boldsymbol{\psi}_2^{\mathrm{RT}_1}) = 0$, one has $A\vec{c} = 0$ and further $\vec{c} = 0$, which demonstrates that $\boldsymbol{\psi}_1^{\mathrm{RT}_1}$ and $\boldsymbol{\psi}_2^{\mathrm{RT}_1}$ are linearly independent (and their divergence also). The second assertion follows from the Gauss theorem and the fact that the constructed functions are normal-trace-free (or alternatively by summing up (2.6) for $k = 1,2,3$). Finally, the bijectivity of the divergence map follows from the orthogonality (to $P_0(T)$) and the linear independence of the divergence of $\boldsymbol{\psi}_1^{\mathrm{RT}_1}$ and $\boldsymbol{\psi}_2^{\mathrm{RT}_1}$.

Proof of (b). Similar calculations as in (a) yield

$$\int_T \mathrm{div}(\varphi_j\boldsymbol{\psi}_j^{\mathrm{RT}_1})\varphi_k \, d\boldsymbol{x} = \frac{3\delta_{jk} - 1}{60} \quad \text{and (with (2.6))} \quad \int_T \mathrm{div}(\boldsymbol{\psi}_j^{\mathrm{RT}_2})\varphi_k \, d\boldsymbol{x} = 0,$$

for $j,k = 1,2,3$. The linear independence and the bijectivity of the divergence map follow from looking at the higher order divergence moments

$$a_{jk} := \int_T \mathrm{div}(\boldsymbol{\psi}_j^{\mathrm{RT}_2})\chi_k \, d\boldsymbol{x} = \frac{4\delta_{jk} - 3}{180} \quad \text{for } j,k = 1,2,3, \tag{2.7}$$

for the three face bubbles $\chi_k = \varphi_{k+1}\varphi_{k-1}$ (the subscript values here should be understood in a circular way). The matrix $A := (a_{jk})_{j,k=1,2,3}$ is nonsingular, since $\det(A) = -\frac{1}{72900}$.

Proof of (c). These statements can be proven in a similar way as in the other cases or simply checked numerically, by computing the necessary matrices on the reference domain. □

Lemma 2.3 (Explicit design of $\boldsymbol{V}_h^{\mathrm{R}}$ for $d = 3$)**.** On any $T \in \mathcal{T}$, the following statements hold:

(a) The functions $\{\boldsymbol{\psi}_j^{\mathrm{RT}_0}\}_{j=1,2,3,4}$ and $\{\boldsymbol{\psi}_j^{\mathrm{RT}_1}\}_{j=1,2,3} \subset \widetilde{\boldsymbol{RT}}_1^{\mathrm{int}}(T)$ are linearly independent. For $\boldsymbol{V}_h^{\mathrm{R}}(T) := \operatorname{span}\{\boldsymbol{\psi}_j^{\mathrm{RT}_0} : j = 1,2,3,4\} \oplus \operatorname{span}\{\boldsymbol{\psi}_j^{\mathrm{RT}_1} : j = 1,2,3\}$ the restricted divergence operator

$$\operatorname{div} : \boldsymbol{V}_h^{\mathrm{R}}(T) \to P_1(T) \quad \text{is surjective (but not bijective).}$$

(b) The functions $\{\boldsymbol{\psi}_j^{\mathrm{RT}_1}\}_{j=1,2,3} \subset \widetilde{\boldsymbol{RT}}_1^{\mathrm{int}}(T)$ and

$$\boldsymbol{\psi}_{(j,k)}^{\mathrm{RT}_2} = (6\varphi_j - 1)\boldsymbol{\psi}_k^{\mathrm{RT}_1} + (6\varphi_k - 1)\boldsymbol{\psi}_j^{\mathrm{RT}_1} \in \widetilde{\boldsymbol{RT}}_2^{\mathrm{int}}(T) \quad \text{for } (j,k) \in \mathcal{S},$$

with $\mathcal{S} = \{(1,2),(1,3),(1,4),(2,3),(2,4),(3,4)\}$ are linearly independent and it holds

$$\int_T \operatorname{div}(\boldsymbol{\psi}_j^{\mathrm{RT}_1})\, d\boldsymbol{x} = 0 \quad \text{for } j = 1,2,3,$$
$$\int_T \operatorname{div}(\boldsymbol{\psi}_{(j,k)}^{\mathrm{RT}_2})\, d\boldsymbol{x} = 0 \quad \text{for } (j,k) \in \mathcal{S}.$$

For $\boldsymbol{V}_h^{\mathrm{R}}(T) := \operatorname{span}\{\boldsymbol{\psi}_j^{\mathrm{RT}_1} : j = 1,2,3\} \oplus \operatorname{span}\{\boldsymbol{\psi}_{(j,k)}^{\mathrm{RT}_2} : (j,k) \in \mathcal{S}\}$ the restricted divergence operator

$$\operatorname{div} : \boldsymbol{V}_h^{\mathrm{R}}(T) \to \widehat{Q}_h^{\perp}(T) \quad \text{for } \widehat{Q}_h(T) = P_0(T) \quad \text{is bijective.}$$

Proof. The proof of this lemma follows the same arguments as the proof in two dimensions. □

3. The full scheme and the uniqueness of its solution

This section formulates the full scheme and discusses the uniqueness of the solution.

3.1. **The scheme.**
Consider the ansatz space

$$\boldsymbol{V}_h := \boldsymbol{V}_h^{\mathrm{ct}} \times \boldsymbol{V}_h^{\mathrm{R}},$$

with $\boldsymbol{V}_h^{\mathrm{ct}} := \boldsymbol{P}_k(\mathcal{T}) \cap \boldsymbol{V}$ and the enrichment space $\boldsymbol{V}_h^{\mathrm{R}} \subset \boldsymbol{H}_0(\operatorname{div},\Omega)$ selected according to the description in Subsection 2.2 (hence either (2.2) or (2.3) holds). Given a function $\boldsymbol{v}_h \in \boldsymbol{V}_h^{\mathrm{ct}} \times \boldsymbol{V}_h^{\mathrm{R}}$ the two components in $\boldsymbol{V}_h^{\mathrm{ct}}$ and $\boldsymbol{V}_h^{\mathrm{R}}$ are denoted by $\boldsymbol{v}_h^{\mathrm{ct}}$ and $\boldsymbol{v}_h^{\mathrm{R}}$, respectively. The pressure space is $Q_h := P_{k-1}^{\mathrm{disc}}(\mathcal{T}) \cap Q$.

Any $\boldsymbol{v}_h^{\mathrm{R}} \in \boldsymbol{V}_h^{\mathrm{R}}$ can be split into

$$\boldsymbol{v}_h^{\mathrm{R}} = \boldsymbol{v}_h^{\mathrm{RT}_0} + \widetilde{\boldsymbol{v}}_h^{\mathrm{R}} = \sum_{F \in \mathcal{F}^0} \operatorname{dof}_F(\boldsymbol{v}_h^{\mathrm{RT}_0})\boldsymbol{\psi}_F + \widetilde{\boldsymbol{v}}_h^{\mathrm{R}} \in \boldsymbol{RT}_0(\mathcal{T}) \oplus \widetilde{\boldsymbol{RT}}_{k-1}^{\mathrm{int}}(\mathcal{T}),$$

where $\boldsymbol{\psi}_F \in \boldsymbol{RT}_0(\mathcal{T})$ is the standard face basis corresponding to $F \in \mathcal{F}^0$ and the operators $\operatorname{dof}_F : \boldsymbol{RT}_0(\mathcal{T}) \to \mathbb{R}, F \in \mathcal{F}^0$, satisfy

$$\operatorname{dof}_F(\boldsymbol{v}_h^{\mathrm{RT}_0}) := \int_F \boldsymbol{v}_h^{\mathrm{RT}_0} \cdot \boldsymbol{n}_F\, ds \Big/ \int_F \boldsymbol{\psi}_F \cdot \boldsymbol{n}_F\, ds \quad \text{for all } \boldsymbol{v}_h^{\mathrm{RT}_0} \in \boldsymbol{RT}_0(\mathcal{T}),$$

with $\boldsymbol{n}_F$ being an unit normal vector of F. For $k = 1$, $\widetilde{\boldsymbol{v}}_h^{\mathrm{R}}$ is always zero; for $k \geqslant d$, $\boldsymbol{v}_h^{\mathrm{RT}_0}$ is always zero.

Define $a(\boldsymbol{u},\boldsymbol{v}) := (\nabla \boldsymbol{u}, \nabla \boldsymbol{v})$ for all $\boldsymbol{u},\boldsymbol{v} \in \boldsymbol{V}$. For $\boldsymbol{v}_h := (\boldsymbol{v}_h^{\mathrm{ct}}, \boldsymbol{v}_h^{\mathrm{R}}) \in \boldsymbol{V}_h^{\mathrm{ct}} \times \boldsymbol{V}_h^{\mathrm{R}}$ consider the (non-symmetric) bilinear form

$$a_h(\boldsymbol{u}_h,\boldsymbol{v}_h) := a(\boldsymbol{u}_h^{\mathrm{ct}},\boldsymbol{v}_h^{\mathrm{ct}}) - (\Delta_{\mathrm{pw}}\boldsymbol{u}_h^{\mathrm{ct}}, \boldsymbol{v}_h^{\mathrm{R}}) + (\Delta_{\mathrm{pw}}\boldsymbol{v}_h^{\mathrm{ct}}, \boldsymbol{u}_h^{\mathrm{R}}) + a_h^D(\boldsymbol{u}_h^{\mathrm{RT}_0}, \boldsymbol{v}_h^{\mathrm{RT}_0}),$$

where Δ_{pw} is the piecewise Laplacian operator with respect to $\mathcal{T}$. Note that the Laplacian terms vanish for $k = 1$, which is the case in [29]. The stabilization $a_h^D : \boldsymbol{RT}_0(\mathcal{T}) \times \boldsymbol{RT}_0(\mathcal{T}) \to \mathbb{R}$ is the same as [29] and has several equivalent choices which satisfy

$$a_h^D(\boldsymbol{v}_h^{\mathrm{RT}_0}, \boldsymbol{v}_h^{\mathrm{RT}_0}) \approx \|\alpha^{1/2} h_{\mathcal{T}}^{-1} \boldsymbol{v}_h^{\mathrm{RT}_0}\|^2, \tag{3.1}$$

where α is a given positive piecewise constant. For simplicity, α is chosen to be constant on the whole domain Ω. In numerical experiments, we choose the form which results in a diagonal block

$$a_h^D(\boldsymbol{u}_h^{\mathrm{RT}_0}, \boldsymbol{v}_h^{\mathrm{RT}_0}) := \alpha \sum_{F \in \mathcal{F}^0} \mathrm{dof}_F(\boldsymbol{u}_h^{\mathrm{RT}_0}) \mathrm{dof}_F(\boldsymbol{v}_h^{\mathrm{RT}_0}) \, (\mathrm{div} \boldsymbol{\psi}_F, \mathrm{div} \boldsymbol{\psi}_F).$$

Note, that the method is stabilization-free for $k \geqslant d$.

Remark 3.1. As in DG methods for elliptic equations (cf. [3]) or for the viscosity term in the Stokes equations (cf. [25, Sec. 4.4]), the second term and the fourth term of a_h are added to guarantee consistency and coercivity, respectively. The choice of the third term can be different. Here, a term which is skew-symmetric to the second term is used. However, one can also employ a symmetric one (i.e., $-(\Delta_{\mathrm{pw}} \boldsymbol{v}_h^{\mathrm{ct}}, \boldsymbol{u}_h^{\mathrm{R}})$). The analysis of the latter case is indeed very similar to the skew-symmetric case except that one should require that α is sufficiently large to guarantee coercivity and a similar stabilization should also be added to the $\widetilde{\boldsymbol{RT}}_{k-1}^{\mathrm{int}}(\mathcal{T})$ part then. The reason for choosing the skew-symmetric form here is that our method is parameter-free in this case for $k \geqslant d$ due to the divergence constraint. The numerical experiments show that this non-symmetry does not affect the convergence rate of the L^2 norm.

On the product space, the bilinear form for the divergence constraint reads

$$b(\boldsymbol{v}_h, q_h) := -(\mathrm{div}(\boldsymbol{v}_h^{\mathrm{ct}} + \boldsymbol{v}_h^{\mathrm{R}}), q_h).$$

The full discrete problem seeks $(\boldsymbol{u}_h, p_h) \in \boldsymbol{V}_h \times Q_h$, such that

$$\begin{aligned} \nu a_h(\boldsymbol{u}_h, \boldsymbol{v}_h) + b(\boldsymbol{v}_h, p_h) &= (\boldsymbol{f}, \boldsymbol{v}_h) \quad \text{for all } \boldsymbol{v}_h \in \boldsymbol{V}_h, \\ b(\boldsymbol{u}_h, q_h) &= 0 \qquad\quad \text{for all } q_h \in Q_h. \end{aligned} \tag{3.2}$$

Here and throughout the rest of the paper, the $\boldsymbol{L}^2$ inner product on the right-hand side is to be understood as

$$(\boldsymbol{f}, \boldsymbol{v}_h) := (\boldsymbol{f}, \boldsymbol{v}_h^{\mathrm{ct}} + \boldsymbol{v}_h^{\mathrm{R}}).$$

In the space of discretely divergence-free functions

$$\begin{aligned} \boldsymbol{V}_{h,0} &:= \left\{ \boldsymbol{v}_h = (\boldsymbol{v}_h^{\mathrm{ct}}, \boldsymbol{v}_h^{\mathrm{R}}) \in \boldsymbol{V}_h : b(\boldsymbol{v}_h, q_h) = 0 \text{ for all } q_h \in Q_h \right\} \\ &= \left\{ \boldsymbol{v}_h = (\boldsymbol{v}_h^{\mathrm{ct}}, \boldsymbol{v}_h^{\mathrm{R}}) \in \boldsymbol{V}_h : \mathrm{div}(\boldsymbol{v}_h^{\mathrm{ct}} + \boldsymbol{v}_h^{\mathrm{R}}) = 0 \right\}, \end{aligned}$$

the above problem is also equivalent to

$$\nu a_h(\boldsymbol{u}_h, \boldsymbol{v}_h) = (\boldsymbol{f}, \boldsymbol{v}_h) \quad \text{for all } \boldsymbol{v}_h \in \boldsymbol{V}_{h,0}. \tag{3.3}$$

Note, that a_h can be naturally extended to $a_h : (\boldsymbol{V} \times \boldsymbol{V}_h^{\mathrm{R}}) \times (\boldsymbol{V} \times \boldsymbol{V}_h^{\mathrm{R}}) \to \mathbb{R}$ and similarly for b. We introduce two seminorms $|||\bullet|||$ and $|||\bullet|||_\star$ on $\boldsymbol{V} \times \boldsymbol{V}_h^{\mathrm{R}}$ which are characterized by

$$|||\boldsymbol{v}|||^2 := a_h(\boldsymbol{v}, \boldsymbol{v}) \quad \text{and} \quad |||\boldsymbol{v}|||_\star^2 := |||\boldsymbol{v}|||^2 + \|h_{\mathcal{T}} \Delta_{\mathrm{pw}} \boldsymbol{v}^{\mathrm{ct}}\|^2 + \|\mathrm{div}(\widetilde{\boldsymbol{v}}^{\mathrm{R}})\|^2, \tag{3.4}$$

for all $\boldsymbol{v} =: (\boldsymbol{v}^{\mathrm{ct}}, \boldsymbol{v}^{\mathrm{R}}) =: (\boldsymbol{v}^{\mathrm{ct}}, \boldsymbol{v}^{\mathrm{RT}_0} + \widetilde{\boldsymbol{v}}^{\mathrm{R}}) \in \boldsymbol{V} \times \boldsymbol{V}_h^{\mathrm{R}}$, respectively.

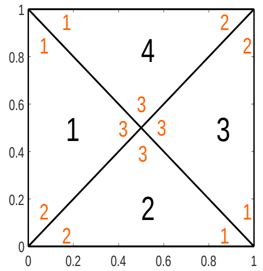

FIGURE 3.1. A mesh of $(0,1)\times(0,1)$. Orange numbers denote the local series number of vertices, and black numbers denote the element series number.

Lemma 3.2. $|||\bullet|||$ is a norm on $\boldsymbol{V}_{h,0}$.

Proof. It suffices to prove that

$$a_h(\boldsymbol{v}_h,\boldsymbol{v}_h)=0 \Rightarrow \boldsymbol{v}_h^{\mathrm{ct}}=\boldsymbol{v}_h^{\mathrm{R}}=\boldsymbol{v}_h^{\mathrm{RT}_0}+\widetilde{\boldsymbol{v}}_h^{\mathrm{R}}=\boldsymbol{0}.$$

Consider $\boldsymbol{v}_h\in\boldsymbol{V}_{h,0}$ with $0=a_h(\boldsymbol{v}_h,\boldsymbol{v}_h)=\|\nabla\boldsymbol{v}_h^{\mathrm{ct}}\|^2+\|\boldsymbol{v}_h^{\mathrm{RT}_0}\|_D^2$, where $\|\bullet\|_D$ is a natural norm on $\boldsymbol{RT}_0(\mathcal{T})\cap\boldsymbol{H}_0(\mathrm{div},\Omega)$ from $a_h^D(\bullet,\bullet)$.

First, $\|\nabla\bullet\|$ and $\|\bullet\|_D$ being norms implies $\boldsymbol{v}_h^{\mathrm{ct}}=\boldsymbol{v}_h^{\mathrm{RT}_0}=\boldsymbol{0}$.

Second, since also $\mathrm{div}(\boldsymbol{v}_h)=\mathrm{div}(\boldsymbol{v}_h^{\mathrm{ct}})+\mathrm{div}(\boldsymbol{v}_h^{\mathrm{RT}_0})+\mathrm{div}(\widetilde{\boldsymbol{v}}_h^{\mathrm{R}})=0$, we have $\mathrm{div}(\widetilde{\boldsymbol{v}}_h^{\mathrm{R}})=0$ and by injectivity of $\mathrm{div}|_{\widetilde{\boldsymbol{RT}}_{k-1}^{\mathrm{int}}(\mathcal{T})}$ it follows $\widetilde{\boldsymbol{v}}_h^{\mathrm{R}}=\boldsymbol{0}$ also. This completes the proof. □

Lemma 3.3. $|||\bullet|||_\star$ is a norm on $\boldsymbol{V}\times\boldsymbol{V}_h^{\mathrm{R}}$.

Proof. The additional term $\|\mathrm{div}(\widetilde{\boldsymbol{v}}^{\mathrm{R}})\|^2$ implies $\mathrm{div}(\widetilde{\boldsymbol{v}}^{\mathrm{R}})=0$ also for any $\boldsymbol{v}\in\boldsymbol{V}\times\boldsymbol{V}_h^{\mathrm{R}}$ if $|||\boldsymbol{v}|||_\star=0$. Then Lemma 3.3 follows with a similar analysis as in Lemma 3.2. □

Note that the two norms are equivalent on $\boldsymbol{V}_{h,0}$ due to an inverse inequality and $\mathrm{div}(\widetilde{\boldsymbol{v}}_h^{\mathrm{R}})=-\mathrm{div}(\boldsymbol{v}_h^{\mathrm{ct}})-\mathrm{div}(\boldsymbol{v}_h^{\mathrm{RT}_0})$ for $\boldsymbol{v}_h\in\boldsymbol{V}_{h,0}$. The Laplacian term in $|||\bullet|||_\star$ is mainly introduced to prove the boundedness of a_h on $(\boldsymbol{V}\times\boldsymbol{V}_h^{\mathrm{R}})\times(\boldsymbol{V}\times\boldsymbol{V}_h^{\mathrm{R}})$.

Remark 3.4 (Remark on uniqueness)**.** It has to be stressed that, apart from the lowest-order case as shown in [29], the spaces $\boldsymbol{V}_h^{\mathrm{ct}}$ and $\boldsymbol{V}_h^{\mathrm{R}}$ might have a non-zero intersection. That means there might be some functions $\boldsymbol{w}\in\boldsymbol{V}_h^{\mathrm{ct}}\cap\boldsymbol{V}_h^{\mathrm{R}}$ which can be represented by $(\beta\boldsymbol{w},(1-\beta)\boldsymbol{w})$ for arbitrary $\beta\in\mathbb{R}$ in the product space $\boldsymbol{V}_h^{\mathrm{ct}}\times\boldsymbol{V}_h^{\mathrm{R}}$. Such an example can be found, e.g., for $k=2$ on a partition as in Fig. 3.1. It is not difficult to verify that $\varphi_3\boldsymbol{\psi}_3^{\mathrm{RT}_0}\in\boldsymbol{V}_h^{\mathrm{R}}$ is also in $\boldsymbol{V}_h^{\mathrm{ct}}$, because $\boldsymbol{\psi}_3^{\mathrm{RT}_0}=2(\boldsymbol{x}-\boldsymbol{m})$ on the whole domain with $\boldsymbol{m}=(0.5,0.5)^\top$ (which is certainly continuous) and φ_3 is continuous with vanishing boundary value. However, if a solution exists (which is proven also later) our method selects a unique representation in $\boldsymbol{V}_{h,0}$ according to Lemma 3.2.

4. Inf-sup stability

This section proves the inf-sup stability of the proposed method for which we assume inf-sup stability of $\boldsymbol{V}_h^{\mathrm{ct}}\times\widehat{Q}_h$ for some auxiliary pressure space $\widehat{Q}_h$ as explained in Subsection 2.2. We first introduce two operators $\mathcal{R}:\boldsymbol{V}\to\boldsymbol{V}_h^{\mathrm{R}}\cap\widetilde{\boldsymbol{RT}}_{k-1}^{\mathrm{int}}(\mathcal{T})$ and $\widetilde{\mathcal{R}}:Q\to\boldsymbol{V}_h^{\mathrm{R}}\cap\widetilde{\boldsymbol{RT}}_{k-1}^{\mathrm{int}}(\mathcal{T})$

which are characterized by

$$\operatorname{div}(\widetilde{\mathcal{R}}q) := \pi_{\widehat{Q}_h^\perp \cap \widetilde{P}_{k-1}^{\mathrm{disc}}(\mathcal{T})} q = \begin{cases} \pi_{\widehat{Q}_h^\perp} q & k \geqslant d, \\ \pi_{\widetilde{P}_{k-1}^{\mathrm{disc}}(\mathcal{T})} q & k < d, \end{cases} \quad \text{for all } q \in Q,$$

with $\widetilde{P}_{k-1}^{\mathrm{disc}}(\mathcal{T})$ as defined in (2.1) and

$$\mathcal{R}\boldsymbol{v} := \widetilde{\mathcal{R}}\left(\operatorname{div}(\boldsymbol{v})\right) \quad \text{for all } \boldsymbol{v} \in \boldsymbol{V}.$$

Due to the bijective property of the divergence operator with respect to the corresponding spaces, these two operators are well-defined. From the definition of $\mathcal{R}$ and $\widetilde{\mathcal{R}}$ one has

$$\operatorname{div}(\mathcal{R}\boldsymbol{v}) = \pi_{\widehat{Q}_h^\perp \cap \widetilde{P}_{k-1}^{\mathrm{disc}}(\mathcal{T})} \operatorname{div}(\boldsymbol{v}). \tag{4.1}$$

Meanwhile, according to the stability of L^2 projection, we have

$$\|\operatorname{div}(\widetilde{\mathcal{R}}q)\| \leqslant \|q\| \quad \text{and} \quad \|\operatorname{div}(\mathcal{R}\boldsymbol{v})\| \leqslant \|\operatorname{div}(\boldsymbol{v})\| \leqslant \|\nabla \boldsymbol{v}\| \quad \text{for all } q \in Q, \boldsymbol{v} \in \boldsymbol{V}. \tag{4.2}$$

4.1. **Fortin operator.** Due to the inf-sup stability of $(\boldsymbol{V}_h^{\mathrm{ct}}, \widehat{Q}_h)$, there exists an $\boldsymbol{H}^1$-stable Fortin operator $\Pi^{\mathrm{ct}} : \boldsymbol{V} \to \boldsymbol{V}_h^{\mathrm{ct}}$, i.e.,

$$\|\nabla \Pi^{\mathrm{ct}} \boldsymbol{v}\| \leqslant C_{\mathrm{F}}^{\mathrm{ct}} \|\nabla \boldsymbol{v}\|, \tag{4.3}$$

and

$$(\operatorname{div}(\Pi^{\mathrm{ct}} \boldsymbol{v}), q_h) = (\operatorname{div}(\boldsymbol{v}), q_h) \quad \text{for all } q_h \in \widehat{Q}_h. \tag{4.4}$$

In cases where $\widehat{Q}_h = \{0\}$, a quasi-interpolation operator Π^{ct}, e.g. the one from [8, Section 4.8], is chosen, which satisfies

$$\|\boldsymbol{v} - \Pi^{\mathrm{ct}} \boldsymbol{v}\|_T \lesssim h_T \|\nabla \boldsymbol{v}\|_{\omega(T)} \quad \text{for all } T \in \mathcal{T}, \boldsymbol{v} \in \boldsymbol{V}, \tag{4.5}$$

with $\omega(T)$ being the union of all nodal patches of vertices in T [26].

Lemma 4.1. The operator $\Pi : \boldsymbol{V} \to \boldsymbol{V}_h$ defined by

$$\Pi \boldsymbol{v} := \begin{cases} \left(\Pi^{\mathrm{ct}} \boldsymbol{v}, \mathcal{R}\widehat{\boldsymbol{v}}\right) & k \geqslant d, \\ \left(\Pi^{\mathrm{ct}} \boldsymbol{v}, \Pi^{\mathrm{RT}_0} \widehat{\boldsymbol{v}} + \mathcal{R}\widehat{\boldsymbol{v}}\right) & k < d, \end{cases} \quad \text{for all } \boldsymbol{v} \in \boldsymbol{V},$$

is a Fortin operator, i.e.,

$$|||\Pi \boldsymbol{v}|||_\star \leqslant C_F \|\nabla \boldsymbol{v}\| \quad \text{and} \quad b(\Pi \boldsymbol{v}, q_h) = -(\operatorname{div}(\boldsymbol{v}), q_h) \quad \text{for all } \boldsymbol{v} \in \boldsymbol{V}, q_h \in Q_h,$$

where $\widehat{\boldsymbol{v}} := (1 - \Pi^{\mathrm{ct}})\boldsymbol{v}$ and Π^{RT_0} is the standard lowest-order Raviart–Thomas interpolation.

Proof. Recall the approximation property of Π^{RT_0} [7],

$$\|\boldsymbol{v} - \Pi^{\mathrm{RT}_0} \boldsymbol{v}\|_T \lesssim h_T \|\nabla \boldsymbol{v}\|_T \quad \text{for all } T \in \mathcal{T}, \boldsymbol{v} \in \boldsymbol{V}. \tag{4.6}$$

Note that (4.2) and (4.3) yield

$$\|\operatorname{div}(\mathcal{R}\widehat{\boldsymbol{v}})\| \leqslant \|\operatorname{div}(\widehat{\boldsymbol{v}})\| \leqslant \|\operatorname{div}(\boldsymbol{v})\| + \|\operatorname{div}(\Pi^{\mathrm{ct}} \boldsymbol{v})\| \leqslant (1 + C_{\mathrm{F}}^{\mathrm{ct}}) \|\nabla \boldsymbol{v}\|.$$

For $k < d$, (4.5) and (4.6) show

$$h_T^{-1} \|\Pi^{\mathrm{RT}_0} \widehat{\boldsymbol{v}}\|_T \lesssim h_T^{-1} \|\widehat{\boldsymbol{v}}\|_T + \|\nabla \widehat{\boldsymbol{v}}\|_T \lesssim \|\nabla \boldsymbol{v}\|_{\omega(T)} + \|\nabla \Pi^{\mathrm{ct}} \boldsymbol{v}\|_T.$$

Then the stability property

$$|||\Pi \boldsymbol{v}|||_\star \lesssim \left(|||\Pi \boldsymbol{v}|||^2 + \|\operatorname{div}(\mathcal{R}\widehat{\boldsymbol{v}})\|^2\right)^{1/2} \lesssim \|\nabla \boldsymbol{v}\|$$

follows from an inverse inequality, (4.3) and the above two inequalities.

Let us prove $b(\Pi\boldsymbol{v}, q_h) = -(\operatorname{div}(\boldsymbol{v}), q_h)$ for all $q_h \in Q_h$. For $k \geqslant d$ and for any $q_h \in Q_h$, due to $\operatorname{div}(\mathcal{R}\widehat{\boldsymbol{v}}) = \pi_{\widehat{Q}_h^\perp}\operatorname{div}(\widehat{\boldsymbol{v}})$ by (4.1) it holds

$$(\operatorname{div}(\mathcal{R}\widehat{\boldsymbol{v}}), q_h) = \left(\pi_{\widehat{Q}_h^\perp}\operatorname{div}(\widehat{\boldsymbol{v}}), \pi_{\widehat{Q}_h^\perp} q_h\right) = \left(\operatorname{div}\left(\boldsymbol{v} - \Pi^{\mathrm{ct}}\boldsymbol{v}\right), \pi_{\widehat{Q}_h^\perp} q_h\right),$$

which implies that

$$\begin{aligned} b(\Pi\boldsymbol{v}, q_h) &= -\left(\operatorname{div}\left(\Pi^{\mathrm{ct}}\boldsymbol{v}\right), \pi_{\widehat{Q}_h} q_h\right) - \left(\operatorname{div}\left(\Pi^{\mathrm{ct}}\boldsymbol{v}\right), \pi_{\widehat{Q}_h^\perp} q_h\right) \\ &\quad - \left(\operatorname{div}\left(\boldsymbol{v} - \Pi^{\mathrm{ct}}\boldsymbol{v}\right), \pi_{\widehat{Q}_h^\perp} q_h\right) \\ (\text{by } (4.4)) \quad &= -\left(\operatorname{div}(\boldsymbol{v}), \pi_{\widehat{Q}_h} q_h\right) - \left(\operatorname{div}(\boldsymbol{v}), \pi_{\widehat{Q}_h^\perp} q_h\right) = -(\operatorname{div}(\boldsymbol{v}), q_h). \end{aligned}$$

For $k < d$, one obtains similarly

$$\left(\operatorname{div}\left(\Pi^{\mathrm{RT}_0}\widehat{\boldsymbol{v}}\right), q_h\right) = \left(\operatorname{div}\left(\boldsymbol{v} - \Pi^{\mathrm{ct}}\boldsymbol{v}\right), \pi_{P_0^{\mathrm{disc}}(\mathcal{T})} q_h\right),$$

and

$$(\operatorname{div}(\mathcal{R}\widehat{\boldsymbol{v}}), q_h) = \left(\operatorname{div}\left(\boldsymbol{v} - \Pi^{\mathrm{ct}}\boldsymbol{v}\right), \pi_{\widetilde{P}_{k-1}^{\mathrm{disc}}(\mathcal{T})} q_h\right).$$

Then the L^2-orthogonality between P_0^{disc} and $\widetilde{P}_{k-1}^{\mathrm{disc}}$ gives

$$(\operatorname{div}(\mathcal{R}\widehat{\boldsymbol{v}}), q_h) + \left(\operatorname{div}\left(\Pi^{\mathrm{RT}_0}\widehat{\boldsymbol{v}}\right), q_h\right) = \left(\operatorname{div}\left(\boldsymbol{v} - \Pi^{\mathrm{ct}}\boldsymbol{v}\right), q_h\right).$$

It follows from the above equality that

$$b(\Pi\boldsymbol{v}, q_h) = -(\operatorname{div}(\boldsymbol{v}), q_h).$$

This completes the proof. □

The existence of a Fortin interpolator implies that the discrete inf-sup condition holds, which is stated in the following theorem.

Theorem 4.2 (Inf-sup stability)**.** There exists a constant $\beta > 0$ independent of h such that

$$\sup_{\boldsymbol{v}_h \in \boldsymbol{V}_h} \frac{b(\boldsymbol{v}_h, q_h)}{|||\boldsymbol{v}_h|||_\star} \geqslant \beta\|q_h\| \quad \text{for all } q_h \in Q_h.$$

Together with a_h being coercive and bounded on $\boldsymbol{V}_{h,0}$ (see Section 5 below), the discrete problem is well-posed and uniquely solvable. In summary, the Raviart–Thomas enrichment of the Scott–Vogelius pairs leads to inf-sup stable pairs on general shape-regular simplicial grids.

5. A priori error analysis

For the subsequent analysis recall that the bilinear form a_h is extended to $\boldsymbol{V} \times \boldsymbol{V}_h$ and the solution $\boldsymbol{u}$ of (1.2) satisfies

$$a_h((\boldsymbol{u}, \boldsymbol{0}), \boldsymbol{v}_h) = a(\boldsymbol{u}, \boldsymbol{v}_h^{\mathrm{ct}}) - (\Delta\boldsymbol{u}, \boldsymbol{v}_h^{\mathrm{R}}) \quad \text{for any } \boldsymbol{v}_h \in \boldsymbol{V}_h.$$

Lemma 5.1 (Consistency)**.** For the solution $\boldsymbol{u} \in \boldsymbol{V}_0$ of (1.2) with $\Delta\boldsymbol{u} \in \boldsymbol{L}^2(\Omega)$, it holds

$$\nu a_h((\boldsymbol{u}, \boldsymbol{0}), \boldsymbol{v}_h) = (\boldsymbol{f}, \boldsymbol{v}_h) \quad \text{for all } \boldsymbol{v}_h \in \boldsymbol{V}_{h,0}.$$

Moreover, if $\boldsymbol{u} \in \boldsymbol{V}_h^{\mathrm{ct}}$ then it is $\boldsymbol{u}_h = (\boldsymbol{u}, \boldsymbol{0})$.

Proof. The first statement follows from

$$\nu a_h((\boldsymbol{u},\mathbf{0}),\boldsymbol{v}_h) = \nu(\nabla\boldsymbol{u},\nabla\boldsymbol{v}_h^{\text{ct}}) - \nu(\Delta\boldsymbol{u},\boldsymbol{v}_h^{\text{R}}) = -\nu(\Delta\boldsymbol{u},\boldsymbol{v}_h^{\text{ct}}+\boldsymbol{v}_h^{\text{R}}) = (\boldsymbol{f},\boldsymbol{v}_h^{\text{ct}}+\boldsymbol{v}_h^{\text{R}}).$$

If $\boldsymbol{u} \in \boldsymbol{V}_h^{\text{ct}}$, this also shows that $\boldsymbol{u}_h = (\boldsymbol{u},\mathbf{0})$ is a discrete solution and due to unique solvability also the only one. □

Lemma 5.2. The following inequality is valid for $\boldsymbol{v}_h \in \widetilde{\boldsymbol{RT}}_k^{\text{int}}(\mathcal{T})$:

$$\|\boldsymbol{v}_h\|_T \leqslant C h_T \|\text{div}\,(\boldsymbol{v}_h)\|_T \quad \text{for all } T\in\mathcal{T}. \tag{5.1}$$

Proof. Recall that we have required in Subsection 2.1 that all local spaces $\widetilde{\boldsymbol{RT}}_k^{\text{int}}(T)$ are obtained by Piola's transformation from a same reference space, which is denoted by $\widetilde{\boldsymbol{RT}}_k^{\text{int}}(T^{\text{ref}})$ in what follows. Due to the injectivity of the divergence operator, both $\|\bullet\|_{T^{\text{ref}}}$ and $\|\text{div}\bullet\|_{T^{\text{ref}}}$ are norms on $\widetilde{\boldsymbol{RT}}_k^{\text{int}}(T^{\text{ref}})$. Since the dimension of $\widetilde{\boldsymbol{RT}}_k^{\text{int}}(T^{\text{ref}})$ is finite, the two norms are equivalent, i.e., there must be two constants $C_\star$ and $C^\star$ which satisfy

$$C_\star \|\text{div}\,(\hat{\boldsymbol{v}}_h)\|_{T^{\text{ref}}} \leqslant \|\hat{\boldsymbol{v}}_h\|_{T^{\text{ref}}} \leqslant C^\star \|\text{div}\,(\hat{\boldsymbol{v}}_h)\|_{T^{\text{ref}}} \quad \text{for all } \hat{\boldsymbol{v}}_h \in \widetilde{\boldsymbol{RT}}_k^{\text{int}}(T^{\text{ref}}). \tag{5.2}$$

The constants $C_\star$ and $C^\star$ are independent of h since the above inequality is related to reference space only.

For any $\boldsymbol{v}_h \in \widetilde{\boldsymbol{RT}}_k^{\text{int}}(T)$, there exists a corresponding reference function $\hat{\boldsymbol{v}}_h \in \widetilde{\boldsymbol{RT}}_k^{\text{int}}(T^{\text{ref}})$. Then a combination of (5.2) and [7, Eqs. 2.1.75 & 2.1.78] gives (5.1). □

Lemma 5.3 (Coercivity and boundedness of a_h)**.** The bilinear form a_h satisfies

$$a_h(\boldsymbol{v}_h,\boldsymbol{v}_h) = |||\boldsymbol{v}_h|||^2 \gtrsim |||\boldsymbol{v}_h|||_\star^2 \quad \text{for all } \boldsymbol{v}_h \in \boldsymbol{V}_{h,0},$$

and

$$a_h(\boldsymbol{u},\boldsymbol{v}) \lesssim |||\boldsymbol{u}|||_\star |||\boldsymbol{v}|||_\star \quad \text{for all } \boldsymbol{u},\boldsymbol{v} \in \boldsymbol{V}\times\boldsymbol{V}_h^{\text{R}}.$$

Proof. The coercivity of a_h is obvious. Let us prove the boundedness. It follows from the Cauchy–Schwarz inequality and Lemma 5.2 that

$$\begin{aligned} a_h(\boldsymbol{u},\boldsymbol{v}) &= (\nabla\boldsymbol{u}^{\text{ct}},\nabla\boldsymbol{v}^{\text{ct}}) - (\Delta_{\text{pw}}\boldsymbol{u}^{\text{ct}},\boldsymbol{v}^{\text{R}}) + (\Delta_{\text{pw}}\boldsymbol{v}^{\text{ct}},\boldsymbol{u}^{\text{R}}) + a_h^D(\boldsymbol{u}^{\text{RT}_0},\boldsymbol{v}^{\text{RT}_0}) \\ &\leqslant \|\nabla\boldsymbol{u}^{\text{ct}}\|\|\nabla\boldsymbol{v}^{\text{ct}}\| + \|h_{\mathcal{T}}\Delta_{\text{pw}}\boldsymbol{u}^{\text{ct}}\|\|h_{\mathcal{T}}^{-1}\boldsymbol{v}^{\text{R}}\| + \|h_{\mathcal{T}}\Delta_{\text{pw}}\boldsymbol{v}^{\text{ct}}\|\|h_{\mathcal{T}}^{-1}\boldsymbol{u}^{\text{R}}\| \\ &\qquad + a_h^D(\boldsymbol{u}^{\text{RT}_0},\boldsymbol{u}^{\text{RT}_0})^{1/2} a_h^D(\boldsymbol{v}^{\text{RT}_0},\boldsymbol{v}^{\text{RT}_0})^{1/2} \\ &\lesssim |||\boldsymbol{u}|||_\star |||\boldsymbol{v}|||_\star. \end{aligned}$$

This concludes the proof. □

Theorem 5.4 (Pressure-robust a priori velocity error estimate)**.** Denote by $\boldsymbol{u}\in\boldsymbol{V}_0$ and $\boldsymbol{u}_h \in \boldsymbol{V}_{h,0}$ the velocity solutions of (1.2) and (3.2), respectively. Assume $\boldsymbol{u}\in\boldsymbol{H}^{k+1}(\Omega)$. It holds

$$|||(\boldsymbol{u},\mathbf{0})-\boldsymbol{u}_h|||_\star \lesssim \inf_{\boldsymbol{v}_h\in\boldsymbol{V}_{h,0}} |||(\boldsymbol{u},\mathbf{0})-\boldsymbol{v}_h|||_\star \leqslant (1+C_F) \inf_{\boldsymbol{v}_h^{\text{ct}}\in\boldsymbol{V}_h^{\text{ct}}} \|\nabla(\boldsymbol{u}-\boldsymbol{v}_h^{\text{ct}})\| \lesssim h^k|\boldsymbol{u}|_{\boldsymbol{H}^{k+1}(\Omega)}.$$

Here, C_F denotes the stability constant of the Fortin interpolator Π. The above inequality implies

$$||\nabla(\boldsymbol{u}-\boldsymbol{u}_h^{\text{ct}})||^2 + \|h_{\mathcal{T}}^{-1}\boldsymbol{u}_h^{\text{R}}\|^2 \lesssim |||(\boldsymbol{u},\mathbf{0})-\boldsymbol{u}_h|||_\star^2 \leqslant h^{2k}|\boldsymbol{u}|_{\boldsymbol{H}^{k+1}(\Omega)}^2.$$

Proof. Lemma 5.1 yields that

$$a_h((\boldsymbol{u},\boldsymbol{0})-\boldsymbol{u}_h,\boldsymbol{v}_h)=0 \quad \text{for all } \boldsymbol{v}_h\in\boldsymbol{V}_{h,0}.$$

Therefore, it follows from Lemma 5.3 that

$$\begin{aligned}|||\boldsymbol{u}_h-\boldsymbol{v}_h|||_\star^2 &\lesssim a_h(\boldsymbol{u}_h-\boldsymbol{v}_h,\boldsymbol{u}_h-\boldsymbol{v}_h)=a_h((\boldsymbol{u},\boldsymbol{0})-\boldsymbol{v}_h,\boldsymbol{u}_h-\boldsymbol{v}_h)\\ &\lesssim |||(\boldsymbol{u},\boldsymbol{0})-\boldsymbol{v}_h|||_\star|||\boldsymbol{u}_h-\boldsymbol{v}_h|||_\star \quad \text{for any } \boldsymbol{v}_h\in\boldsymbol{V}_{h,0}.\end{aligned}$$

This and a triangle inequality shows

$$||\nabla(\boldsymbol{u}-\boldsymbol{u}_h^{\mathrm{ct}})||\leqslant|||(\boldsymbol{u},\boldsymbol{0})-\boldsymbol{u}_h|||_\star\leqslant|||(\boldsymbol{u},\boldsymbol{0})-\boldsymbol{v}_h|||_\star+|||\boldsymbol{u}_h-\boldsymbol{v}_h|||_\star\lesssim|||(\boldsymbol{u},\boldsymbol{0})-\boldsymbol{v}_h|||_\star.$$

Since $\boldsymbol{v}_h$ is arbitrary, one gets

$$|||(\boldsymbol{u},\boldsymbol{0})-\boldsymbol{u}_h|||_\star\lesssim\inf_{\boldsymbol{v}_h\in\boldsymbol{V}_{h,0}}|||(\boldsymbol{u},\boldsymbol{0})-\boldsymbol{v}_h|||_\star.$$

Consider now $\boldsymbol{w}_h=(\boldsymbol{w}_h^{\mathrm{ct}},0)$ with any $\boldsymbol{w}_h^{\mathrm{ct}}$ in $\boldsymbol{V}_h^{\mathrm{ct}}$ and choose $\boldsymbol{v}_h:=\Pi(\boldsymbol{u}-\boldsymbol{w}_h^{\mathrm{ct}})+\boldsymbol{w}_h\in\boldsymbol{V}_{h,0}$. Due to the properties of the Fortin operator, one obtains

$$|||(\boldsymbol{u},\boldsymbol{0})-\boldsymbol{v}_h|||_\star\leqslant|||(\boldsymbol{u},\boldsymbol{0})-\boldsymbol{w}_h|||_\star+|||\Pi(\boldsymbol{u}-\boldsymbol{w}_h^{\mathrm{ct}})|||_\star\leqslant(1+C_F)\|\nabla(\boldsymbol{u}-\boldsymbol{w}_h^{\mathrm{ct}})\|.$$

Since $\boldsymbol{w}_h^{\mathrm{ct}}$ is arbitrary, this inequality also holds for the infimums on both sides. Hence, one arrives at

$$|||(\boldsymbol{u},\boldsymbol{0})-\boldsymbol{u}_h|||_\star\lesssim(1+C_F)\inf_{\boldsymbol{w}_h^{\mathrm{ct}}\in\boldsymbol{V}_h^{\mathrm{ct}}}\|\nabla(\boldsymbol{u}-\boldsymbol{w}_h^{\mathrm{ct}})\|.$$

This finishes the proof. □

Theorem 5.5 (A priori pressure error estimate)**.** Denote by $p\in Q$ and $p_h\in Q_h$ the pressure solutions of (1.2) and (3.2), respectively. Assume $\boldsymbol{u}\in\boldsymbol{H}^{k+1}(\Omega)$ and $p\in H^k(\Omega)$. It holds

$$\|p-p_h\|\lesssim\inf_{q_h\in Q_h}\|p-q_h\|+\nu|||(\boldsymbol{u},\boldsymbol{0})-\boldsymbol{u}_h|||_\star\lesssim h^k|p|_{H^k(\Omega)}+\nu h^k|\boldsymbol{u}|_{\boldsymbol{H}^{k+1}(\Omega)}.$$

Proof. First, there is an identity for the L^2 best-approximation $\pi_{Q_h}p$ within Q_h, which gives

$$\|p-p_h\|^2=\inf_{q_h\in Q_h}\|p-q_h\|^2+\|\pi_{Q_h}p-p_h\|^2.$$

To estimate the last term, the inf-sup stability guarantees the existence of some $\boldsymbol{v}_h\in\boldsymbol{V}_h$ such that $\operatorname{div}(\boldsymbol{v}_h^{\mathrm{ct}}+\boldsymbol{v}_h^{\mathrm{R}})=\pi_{Q_h}p-p_h$ and $|||\boldsymbol{v}_h|||_\star\lesssim\|\pi_{Q_h}p-p_h\|$. This allows for the estimate

$$\begin{aligned}\|\pi_{Q_h}p-p_h\|^2&=-b(\boldsymbol{v}_h,\pi_{Q_h}p-p_h)=-b(\boldsymbol{v}_h,p-p_h)\\&=\nu a_h((\boldsymbol{u},\boldsymbol{0})-\boldsymbol{u}_h,\boldsymbol{v}_h)\\&\lesssim\nu|||(\boldsymbol{u},\boldsymbol{0})-\boldsymbol{u}_h|||_\star\,|||\boldsymbol{v}_h|||_\star.\end{aligned}$$

Inserting the bound for $|||\boldsymbol{v}_h|||_\star$ concludes the proof. □

6. Reduction to divergence-free schemes with only P_0 pressure

This section derives a reduced scheme that allows to remove the additional Raviart–Thomas degrees of freedom and only requires a P_0 pressure, effectively resulting into a $\boldsymbol{P}_k\times P_0$-like system. Similar reduced schemes can be found in [27, 13, 39]. The idea of our scheme is based on the important fact that the divergence operator from $\widetilde{\boldsymbol{RT}}_{k-1}^{\mathrm{int}}(\mathcal{T})$ to $\widetilde{P}_{k-1}^{\mathrm{disc}}(\mathcal{T})$ is bijective.

Firstly a general framework is given for $k\geqslant d$, where it is shown that our method is equivalent to a computable $\boldsymbol{P}_k\times\widehat{Q}_h$-like system. Then taking $\widehat{Q}_h=P_0^{\mathrm{disc}}(\mathcal{T})\cap Q$ results in a $\boldsymbol{P}_k \times P_0$-like system for arbitrary $k \geqslant d$. The reduced scheme for $k < d$ is seperately discussed.

6.1. **General framework for $k \geqslant d$.** Due to the divergence constraint, there are a series of equivalent reduced schemes which seek the velocity in a subspace of $\boldsymbol{V}_h$. The scheme (3.3) is such an example which is commonly used in theoretical analysis. However, (3.3) is not connected to practical computations in general because the divergence-free basis functions are usually non-trivial to construct. This subsection discusses a computable reduced scheme ($\boldsymbol{P}_k \times \widehat{Q}_h$-like), where the operators $\mathcal{R}$ and $\widetilde{\mathcal{R}}$ play an important role again.

The velocity ansatz space that incorporates the divergence constraint by $\widehat{Q}_h^{\perp}$ reads

$$\widehat{\boldsymbol{V}}_h := \left\{ \boldsymbol{v}_h = (\boldsymbol{v}_h^{\mathrm{ct}}, \boldsymbol{v}_h^{\mathrm{R}}) \in \boldsymbol{V}_h : \int_\Omega \operatorname{div}(\boldsymbol{v}_h^{\mathrm{ct}} + \boldsymbol{v}_h^{\mathrm{R}}) \lambda_h \, d\boldsymbol{x} = 0 \quad \forall \lambda_h \in \widehat{Q}_h^{\perp} \right\}. \tag{6.1}$$

Due to the inclusion relationship $\operatorname{div}(\boldsymbol{V}_h^{\mathrm{ct}} + \boldsymbol{V}_h^{\mathrm{R}}) \subseteq Q_h$ and the L^2-orthogonal relationship between $\widehat{Q}_h$ and $\widehat{Q}_h^{\perp}$, $\widehat{\boldsymbol{V}}_h$ can be also characterized as

$$\widehat{\boldsymbol{V}}_h = \left\{ \boldsymbol{v}_h = (\boldsymbol{v}_h^{\mathrm{ct}}, \boldsymbol{v}_h^{\mathrm{R}}) \in \boldsymbol{V}_h : \operatorname{div}(\boldsymbol{v}_h^{\mathrm{ct}} + \boldsymbol{v}_h^{\mathrm{R}}) \in \widehat{Q}_h \right\}.$$

Then our method is also equivalent to seeking $\boldsymbol{u}_h \in \widehat{\boldsymbol{V}}_h$ and $\hat{p}_h \in \widehat{Q}_h$, such that

$$\begin{aligned} \nu a_h(\boldsymbol{u}_h, \boldsymbol{v}_h) + b(\boldsymbol{v}_h, \hat{p}_h) &= (\boldsymbol{f}, \boldsymbol{v}_h) \quad \text{for all } \boldsymbol{v}_h \in \widehat{\boldsymbol{V}}_h, \\ b(\boldsymbol{u}_h, q_h) &= 0 \qquad\qquad \text{for all } q_h \in \widehat{Q}_h. \end{aligned} \tag{6.2}$$

Lemma 6.1. The following identity holds:

$$\widehat{\boldsymbol{V}}_h = \left\{ \boldsymbol{v}_h = \left(\boldsymbol{v}_h^{\mathrm{ct}}, -\mathcal{R}\boldsymbol{v}_h^{\mathrm{ct}} \right) : \boldsymbol{v}_h^{\mathrm{ct}} \in \boldsymbol{V}_h^{\mathrm{ct}} \right\}.$$

Proof. This proof is based on the L^2-orthogonality between $\widehat{Q}_h$ and $\widehat{Q}_h^{\perp}$. For any $\boldsymbol{v}_h^{\mathrm{ct}} \in \boldsymbol{V}_h^{\mathrm{ct}}$, one has $\operatorname{div}(\boldsymbol{v}_h^{\mathrm{ct}}) + \operatorname{div}(-\mathcal{R}\boldsymbol{v}_h^{\mathrm{ct}}) = \operatorname{div}(\boldsymbol{v}_h^{\mathrm{ct}}) - \pi_{\widehat{Q}_h^{\perp}} \operatorname{div}(\boldsymbol{v}_h^{\mathrm{ct}}) = \pi_{\widehat{Q}_h} \operatorname{div}(\boldsymbol{v}_h^{\mathrm{ct}}) \in \widehat{Q}_h$, which implies that

$$\widehat{\boldsymbol{V}}_h \supseteq \left\{ \boldsymbol{v}_h = \left(\boldsymbol{v}_h^{\mathrm{ct}}, -\mathcal{R}\boldsymbol{v}_h^{\mathrm{ct}} \right) : \boldsymbol{v}_h^{\mathrm{ct}} \in \boldsymbol{V}_h^{\mathrm{ct}} \right\}.$$

Conversely, for any $\boldsymbol{v}_h = (\boldsymbol{v}_h^{\mathrm{ct}}, \boldsymbol{v}_h^{\mathrm{R}}) \in \boldsymbol{V}_h$ which satisfies $\operatorname{div}(\boldsymbol{v}_h^{\mathrm{ct}} + \boldsymbol{v}_h^{\mathrm{R}}) \in \widehat{Q}_h$, it follows from the orthogonality that

$$\left(\operatorname{div}(\boldsymbol{v}_h^{\mathrm{ct}} + \boldsymbol{v}_h^{\mathrm{R}}), q_h \right) = 0 \quad \text{for all } q_h \in \widehat{Q}_h^{\perp}.$$

The above equality means that $\operatorname{div}(\boldsymbol{v}_h^{\mathrm{R}}) = -\pi_{\widehat{Q}_h^{\perp}} \operatorname{div}(\boldsymbol{v}_h^{\mathrm{ct}})$ and further $\boldsymbol{v}_h^{\mathrm{R}}$ is exactly $-\mathcal{R}\boldsymbol{v}_h^{\mathrm{ct}}$, which implies that

$$\widehat{\boldsymbol{V}}_h \subseteq \left\{ \boldsymbol{v}_h = \left(\boldsymbol{v}_h^{\mathrm{ct}}, -\mathcal{R}\boldsymbol{v}_h^{\mathrm{ct}} \right) : \boldsymbol{v}_h^{\mathrm{ct}} \in \boldsymbol{V}_h^{\mathrm{ct}} \right\}.$$

This completes the proof. ☐

According to Lemma 6.1 one can rewrite (6.2) as seeking $\boldsymbol{u}_h^{\mathrm{ct}} \in \boldsymbol{V}_h^{\mathrm{ct}}$ such that

$$\begin{aligned} \nu a_h((\boldsymbol{u}_h^{\mathrm{ct}}, -\mathcal{R}\boldsymbol{u}_h^{\mathrm{ct}}), (\boldsymbol{v}_h^{\mathrm{ct}}, -\mathcal{R}\boldsymbol{v}_h^{\mathrm{ct}})) - (\operatorname{div}(\boldsymbol{v}_h^{\mathrm{ct}}), \hat{p}_h) &= (\boldsymbol{f}, \boldsymbol{v}_h^{\mathrm{ct}} - \mathcal{R}\boldsymbol{v}_h^{\mathrm{ct}}) \quad \text{for all } \boldsymbol{v}_h^{\mathrm{ct}} \in \boldsymbol{V}_h^{\mathrm{ct}}, \\ (\operatorname{div}(\boldsymbol{u}_h^{\mathrm{ct}}), q_h) &= 0 \qquad\qquad\qquad\quad \text{for all } q_h \in \widehat{Q}_h, \end{aligned} \tag{6.3}$$

In this rewriting we apply also the fact that $(\operatorname{div}(\mathcal{R}\boldsymbol{v}_h^{\mathrm{ct}}), q_h) = 0$ for all $(\boldsymbol{v}_h^{\mathrm{ct}}, q_h) \in \boldsymbol{V}_h^{\mathrm{ct}} \times \widehat{Q}_h$.

The scheme (6.3) is the so-called $\boldsymbol{P}_k \times \widehat{Q}_h$-like scheme herein. The implementation of (6.3) relies on the simple implementation of $\mathcal{R}$. Note that $\boldsymbol{V}_h^{\mathrm{R}}$ consists of some interior cell functions. The computation of $\mathcal{R}$ can be done on each element T, and clearly we have $\mathcal{R}\boldsymbol{v}_h^{\mathrm{ct}}|_T = \mathbf{0}$ if $\operatorname{div}(\boldsymbol{v}_h^{\mathrm{ct}})|_T \in \widehat{Q}_h$. Denote by $\{\boldsymbol{\psi}_j, j = 1, ..., N_0\}$ the basis of $\boldsymbol{V}_h^{\mathrm{R}}(T)$, where $N_0 = \dim(\boldsymbol{V}_h^{\mathrm{R}}(T))$. The computation is equivalent to solving a local problem $A_T\boldsymbol{u}_T = \boldsymbol{b}_T$, where

$$A_T := \left(\int_T \operatorname{div}(\boldsymbol{\psi}_j)\operatorname{div}(\boldsymbol{\psi}_k)\,d\boldsymbol{x}\right)_{j,k} \quad \text{and} \quad b_T := \left(\int_T \operatorname{div}(\boldsymbol{v}_h^{\mathrm{ct}})\operatorname{div}(\boldsymbol{\psi}_j)\,d\boldsymbol{x}\right)_j. \tag{6.4}$$

Then $\boldsymbol{u}_T = (u_j) \in \mathbb{R}^{N_0}$ is indeed the vector of coefficients of the expansion of $\mathcal{R}\boldsymbol{v}_h^{\mathrm{ct}}$ on T, i.e., $\mathcal{R}\boldsymbol{v}_h^{\mathrm{ct}}|_T = \sum u_j\boldsymbol{\psi}_j$. Moreover, one even does not need to solve local problems on each element. This computation can be achieved by affine transformation from the unit reference element (see Subsection 6.4 below).

6.2. **The $\boldsymbol{P}_k \times P_0$-like scheme for arbitrary order.** For $k \geqslant d$, taking $\widehat{Q}_h = P_0^{\mathrm{disc}}(\mathcal{T}) \cap Q$ in Subsection 6.1 results in a $\boldsymbol{P}_k \times P_0$-like scheme. For $k < d$, $\widetilde{P}_{k-1}^{\mathrm{disc}}(\mathcal{T})$ and $\widetilde{\boldsymbol{RT}}_{k-1}^{\mathrm{int}}(\mathcal{T})$ play a similar role as $\widehat{Q}_h^{\perp}$ and $\boldsymbol{V}_h^{\mathrm{R}}$ before in Subsection 6.1. Then the corresponding reduced scheme for $k < d$ seeks $\hat{\boldsymbol{u}}_h = (\boldsymbol{u}_h^{\mathrm{ct}}, \boldsymbol{u}_h^{\mathrm{RT}_0}) \in \boldsymbol{V}_h^{\mathrm{ct}} \times (\boldsymbol{RT}_0(\mathcal{T}) \cap \boldsymbol{H}_0(\operatorname{div}, \Omega))$ such that

$$\begin{aligned} \nu a_h(\hat{\boldsymbol{u}}_h - (\mathbf{0}, \mathcal{R}\boldsymbol{u}_h^{\mathrm{ct}}), \hat{\boldsymbol{v}}_h - (\mathbf{0}, \mathcal{R}\boldsymbol{v}_h^{\mathrm{ct}})) + b(\hat{\boldsymbol{v}}_h, \hat{p}_h) &= (\boldsymbol{f}, \hat{\boldsymbol{v}}_h - (\mathbf{0}, \mathcal{R}\boldsymbol{v}_h^{\mathrm{ct}})), \\ b(\hat{\boldsymbol{u}}_h, q_h) &= 0, \end{aligned} \tag{6.5}$$

for all $\hat{\boldsymbol{v}}_h = (\boldsymbol{v}_h^{\mathrm{ct}}, \boldsymbol{v}_h^{\mathrm{RT}_0}) \in \boldsymbol{V}_h^{\mathrm{ct}} \times (\boldsymbol{RT}_0(\mathcal{T}) \cap \boldsymbol{H}_0(\operatorname{div}, \Omega)), q_h \in P_0^{\mathrm{disc}}(\mathcal{T}) \cap Q$. Note that (6.5) can be further reduced to a $\boldsymbol{P}_k \times P_0$ system, after removing the $\boldsymbol{RT}_0$ unknowns by static condensation since the $\boldsymbol{RT}_0 - \boldsymbol{RT}_0$ block is diagonal [29].

Here, $\boldsymbol{V}_h^{\mathrm{R}}$ should be chosen as

$$\boldsymbol{V}_h^{\mathrm{R}} := \begin{cases} \widetilde{\boldsymbol{RT}}_{k-1}^{\mathrm{int}}(\mathcal{T}) & k \geqslant d, \\ (\boldsymbol{RT}_0(\mathcal{T}) \cap \boldsymbol{H}_0(\operatorname{div}, \Omega)) \oplus \widetilde{\boldsymbol{RT}}_{k-1}^{\mathrm{int}}(\mathcal{T}) & k < d. \end{cases}$$

Indeed, this approach results in the same space as in Tables 2.1 and 2.2 for $k \leqslant d$ but in a larger space for $k \geqslant d+1$. For $k = 3, 4$ in two dimensions, $\widetilde{\boldsymbol{RT}}_{k-1}^{\mathrm{int}}(\mathcal{T})$ is exactly the sum of the chosen Raviart–Thomas subspaces from 2 to k in Table 2.1.

Remark 6.2. For a general order k, one can also use the non-divergence-free interior shape functions in [27, § 2.2.4] (two dimensions) and [40, pp. 106–107] (three dimensions), which forms a subspace of the Brezzi–Douglas–Marini spaces of order k, isomorphic to $\widetilde{\boldsymbol{RT}}_{k-1}^{\mathrm{int}}(\mathcal{T})$, and makes the divergence operator bijective onto $\widetilde{P}_{k-1}^{\mathrm{disc}}(\mathcal{T})$. This subspace fulfills all the properties needed in our methods and plays a similar role as $\widetilde{\boldsymbol{RT}}_{k-1}^{\mathrm{int}}(\mathcal{T})$.

6.3. **Recovering $\tilde{p}_h = p_h - \hat{p}_h$ locally on each element T.** For simplicity, we use $k \geqslant d$ as an example. Due to the inf-sup stability of $(\boldsymbol{V}_h^{\mathrm{ct}}, \widehat{Q}_h)$, it holds that $\pi_{\widehat{Q}_h}\operatorname{div}(\boldsymbol{V}_h^{\mathrm{ct}}) = \widehat{Q}_h$ and further $\operatorname{div}(\widehat{\boldsymbol{V}}_h) = \widehat{Q}_h$. Meanwhile, since $\widehat{\boldsymbol{V}}_h$ is a subspace of $\boldsymbol{V}_h$, the full pressure p_h also satisfies

$$\nu a_h(\boldsymbol{u}_h, \boldsymbol{v}_h) + b(\boldsymbol{v}_h, p_h) = (\boldsymbol{f}, \boldsymbol{v}_h) \quad \text{for all } \boldsymbol{v}_h \in \widehat{\boldsymbol{V}}_h. \tag{6.6}$$

Subtracting (6.6) from (6.2) one gets, for all $\boldsymbol{v}_h \in \widehat{\boldsymbol{V}}_h$,

$$b(\boldsymbol{v}_h, p_h) = b(\boldsymbol{v}_h, \hat{p}_h),$$

which implies $\hat{p}_h = \pi_{\widehat{Q}_h}p_h$ and $\tilde{p}_h = p_h - \hat{p}_h \in \widehat{Q}_h^{\perp}$.

Now let us introduce the recover method for p_h on $T \in \mathcal{T}$. Like Subsection 6.1, let $\{\boldsymbol{\psi}_j, j = 1, \ldots, N_0\}$ be the set of basis functions of $\boldsymbol{V}_h^{\mathrm{R}}$. Note also that $\mathrm{div}(\boldsymbol{\psi}_j), j = 1, \ldots, N_0$, are linearly independent and

$$\mathrm{span}\left\{\mathrm{div}(\boldsymbol{\psi}_j), j = 1, ..., N_0\right\} = \widehat{Q}_h^{\perp}(T),$$

by bijectivity of $\mathrm{div}|_{\boldsymbol{V}_h^{\mathrm{R}}}$. Hence the following equations form a local problem for $\tilde{p}_h$ on T:

$$(\tilde{p}_h, \mathrm{div}(\boldsymbol{\psi}_j))_T = -(\boldsymbol{f}, \boldsymbol{\psi}_j)_T + \nu a_h(\boldsymbol{u}_h, (\boldsymbol{0}, \boldsymbol{\psi}_j))_T, \quad j = 1, \ldots, N_0.$$

The above system forms the matrix A_T also if one uses $\{\mathrm{div}\boldsymbol{\psi}_j\}$ as the basis for representing $\tilde{p}_h$.

6.4. **Implementation.** This subsection comments on the algebraic structure of the full and the reduced scheme and some remarks on the efficient implementation. Algebraically the full scheme solves a system of the form

$$\begin{pmatrix} A_{\mathrm{cc}} & A_{\mathrm{Rc}}^{\top} & B_{\mathrm{c}}^{\top} \\ -A_{\mathrm{Rc}} & A_{\mathrm{RR}} & B_{\mathrm{R}}^{\top} \\ B_{\mathrm{c}} & B_{\mathrm{R}} & 0 \end{pmatrix} \begin{pmatrix} U_{\mathrm{c}} \\ U_{\mathrm{R}} \\ P \end{pmatrix} = \begin{pmatrix} F_{\mathrm{c}} \\ F_{\mathrm{R}} \\ 0 \end{pmatrix},$$

where U_{c}, U_{R}, and P are the coefficients for $\boldsymbol{V}_h^{\mathrm{ct}}$, $\boldsymbol{V}_h^{\mathrm{R}}$ and Q_h, respectively. The blocks A_{cc}, B_{c}, F_{c} are the standard blocks related to a and b and $\boldsymbol{f}$, respectively. The blocks B_{R}, F_{R} represent the b and $\boldsymbol{f}$ applied to functions from $\boldsymbol{V}_h^{\mathrm{R}}$. The stabilization block A_{RR} refers to a_h^D and is only needed when $k < d$. In the lowest-order case $k = 1$ it holds $A_{\mathrm{Rc}} = 0$, but for $k > 1$ it corresponds to $(\Delta_{\mathrm{pw}}\boldsymbol{u}_h^{\mathrm{ct}}, \boldsymbol{v}_h^{\mathrm{R}})$.

For brevity, we restrict the remaining presentation to the case $k \geqslant d$, such that no $\boldsymbol{RT}_0$ part is involved. Given a representation matrix R for the linear mapping $\mathcal{R} : \boldsymbol{V}_h^{\mathrm{ct}} \to \boldsymbol{V}_h^{\mathrm{R}}$ from the previous section, the reduced scheme solves instead the much smaller system

$$\begin{pmatrix} A_{\mathrm{cc}} - A_{\mathrm{Rc}}^{\top}R + R^{\top}A_{\mathrm{Rc}} & B_0^{\top} \\ B_0 & 0 \end{pmatrix} \begin{pmatrix} U_{\mathrm{c}} \\ P_0 \end{pmatrix} = \begin{pmatrix} F_{\mathrm{c}} - R^{\top}F_{\mathrm{R}} \\ 0 \end{pmatrix},$$

where U_{c} and P_0 are the coefficients for $\boldsymbol{V}_h^{\mathrm{ct}}$ and $P_0^{\mathrm{disc}}(\mathcal{T}) \cap Q$, respectively. The Raviart–Thomas part can be recovered by $U_{\mathrm{R}} = -RU_{\mathrm{c}}$.

Next, an efficient assembly of the representation matrix R will be explained. It is sparse and can be computed by solving local problems for each degree of freedom on each cell $T \in \mathcal{T}$. In fact, for each basis function $\boldsymbol{v}_j^{\mathrm{ct}} \in \boldsymbol{V}_h^{\mathrm{ct}}$ with support in $T \in \mathcal{T}$, one has to solve a system formed by (6.4), and to add the solution to the j-th row of R.

These solutions can be obtained very efficiently via the following strategy. Assume $k = 2$ in two dimensions as an example. We compute $\mathcal{R}$ via $\widetilde{\mathcal{R}}$ by the relationship $\mathcal{R}\boldsymbol{v}_h^{\mathrm{ct}} = \widetilde{\mathcal{R}}(\mathrm{div}\boldsymbol{v}_h^{\mathrm{ct}})$ for all $\boldsymbol{v}_h^{\mathrm{ct}} \in \boldsymbol{V}_h^{\mathrm{ct}}$. Note that $\mathrm{div}\boldsymbol{V}_h^{\mathrm{ct}}|_T \subseteq P_1(T) = \mathrm{span}\{\varphi_1, \varphi_2, \varphi_3\}$ and a nodal interpolation allows to determine the coefficients c_j in $\mathrm{div}\boldsymbol{v}_h^{\mathrm{ct}} = \sum c_j\varphi_j$. Hence the problem reduces to find the images of $\widetilde{\mathcal{R}}(\varphi_j|_T) = \sum_{j=1}^{3} x_{T,j}\boldsymbol{\psi}_j^{\mathrm{RT}_1}$ for $j = 1, 2, 3$ and the particular basis functions $\boldsymbol{\psi}_j^{\mathrm{RT}_1}$ on T. In principle one needs to solve the linear system of equations $A_T\boldsymbol{x}_{T,j} = \boldsymbol{b}_{T,j}$ with A_T from (6.4) and

$$\boldsymbol{b}_{T,j} := \left(\int_T \varphi_j \mathrm{div}(\boldsymbol{\psi}_k^{\mathrm{RT}_1})\, d\boldsymbol{x}\right)_{k=1,2,3}.$$

However, employing the properties of the standard (Piola) transformations between the reference simplex T^{ref} and the general simplex T, see ,e.g., [7, Chapter II, §2] for details, it holds $A_T = J^{-1}A_{T^{\mathrm{ref}}}$ and $\boldsymbol{b}_{T,j} = \boldsymbol{b}_{T^{\mathrm{ref}},j}$ where J is the determinant of the matrix of the

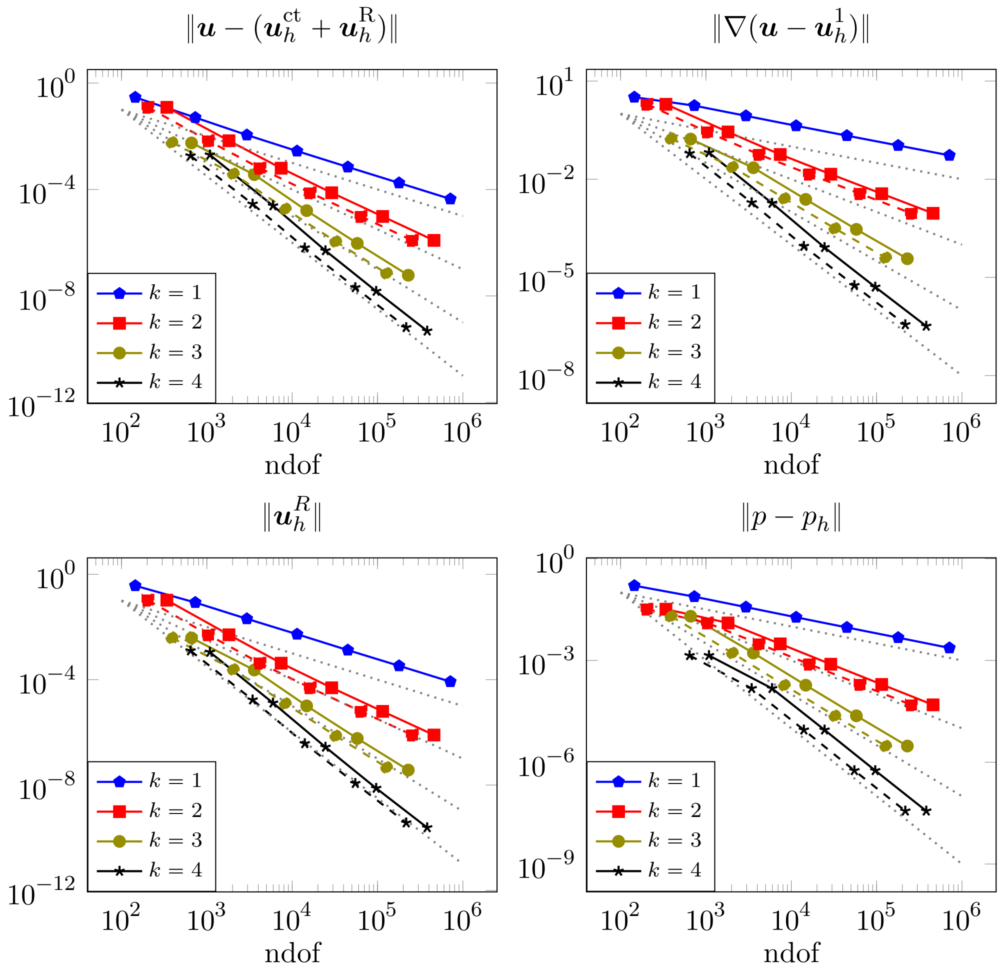

FIGURE 7.1. Example 1: Convergence history for $\|\boldsymbol{u} - (\boldsymbol{u}_h^{\mathrm{ct}} + \boldsymbol{u}_h^{\mathrm{R}})\|$ (top left), $\|\nabla(\boldsymbol{u} - \boldsymbol{u}_h^1)\|$ (top right), $\|\boldsymbol{u}^R\|$ (bottom left), and $\|p - p_h\|$ (bottom right) for different k. The solid lines coresspond to the full schemes, while dashed lines coresspond to the reduced schemes. The slopes of the gray dotted lines coresspond to the expected optimal order of the curve(s) right above them.

affine transformation, i.e., $J = d!|T|$. In other words, it holds $\boldsymbol{x}_{T,j} = J\boldsymbol{x}_{T^{\mathrm{ref}},j}$ and the local systems for $j = 1, 2, 3$ only have to be solved once on the reference domain. Of course, the process can be generalized to larger k.

Similarly, for the pressure recovering process, one has $A_T^{-1} = JA_{T^{\mathrm{ref}}}^{-1}$. Thus we only need to solve the inverse of $A_{T^{\mathrm{ref}}}$ and all inverses of A_T can be obtained from it directly. Then the process of pressure recovering only requires matrix-vector multiplications.

7. Numerical results

This section confirms the theoretical findings in two numerical examples. For $k < d$, the lowest-order Raviart–Thomas part is stabilized with $\alpha = 1$ in all numerical studies.

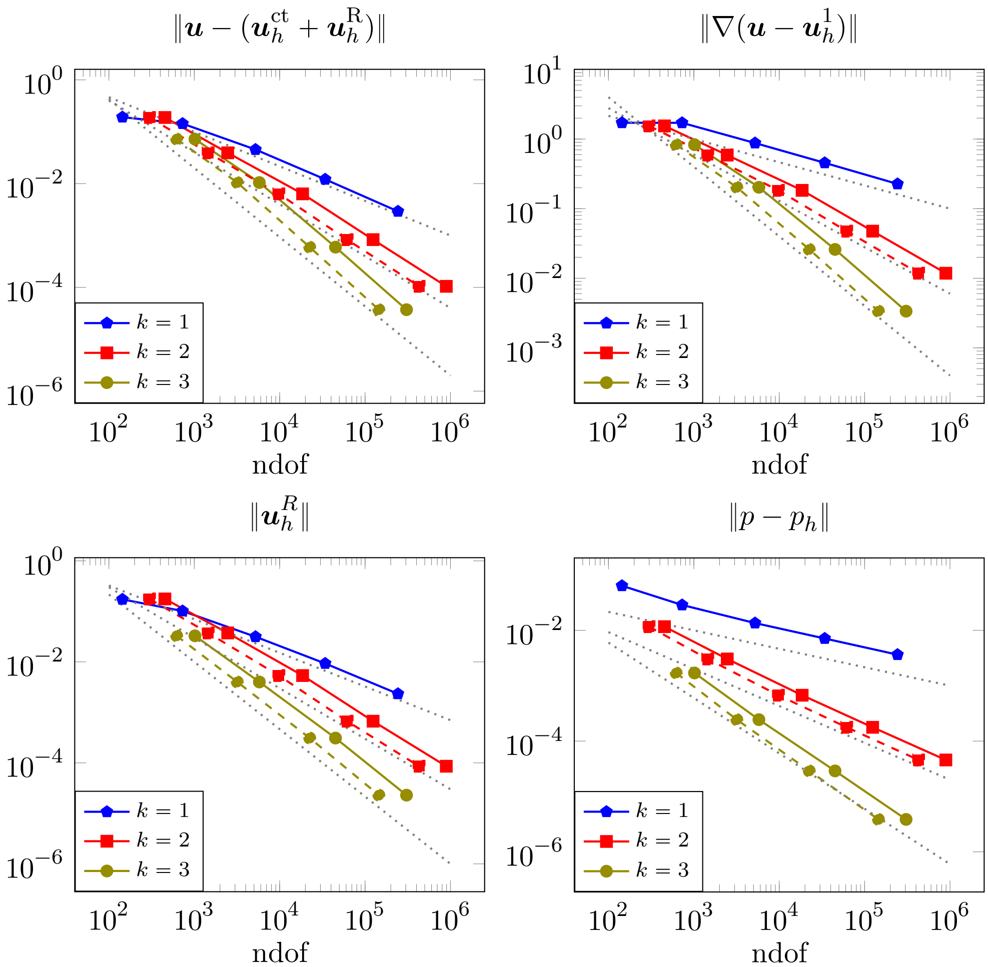

FIGURE 7.2. Example 2: Convergence history for $\|\boldsymbol{u} - (\boldsymbol{u}_h^{\mathrm{ct}} + \boldsymbol{u}_h^{\mathrm{R}})\|$ (top left), $\|\nabla(\boldsymbol{u} - \boldsymbol{u}_h^1)\|$ (top right), $\|\boldsymbol{u}^R\|$ (bottom left), and $\|p - p_h\|$ (bottom right) for different k. The solid lines coresspond to the full schemes, while dashed lines coresspond to the reduced schemes. The slopes of the gray dotted lines coresspond to the expected optimal order of the curve(s) right above them.

7.1. **Example 1 - Two-dimensional planar lattice flow.** Consider the planar lattice flow

$$\boldsymbol{u} = \begin{pmatrix} \sin(2\pi x)\sin(2\pi y) \\ \cos(2\pi x)\cos(2\pi y) \end{pmatrix} \quad \text{and} \quad p = (\cos(4\pi x) - \cos(4\pi y))/4$$

with $\boldsymbol{f}$ chosen such that $(\boldsymbol{u}, p)$ solves the Stokes problem with $\nu = 10^{-3}$.

Figure 7.1 displays the convergence histories for the velocity and pressure errors and confirms that all methods converge optimally for order $k = 1, 2, 3, 4$ according to Theorems 5.4 and 5.5. Further studies, which are not presented for the sake of brevity, showed also that $\boldsymbol{u}_h^{\mathrm{ct}} + \boldsymbol{u}_h^{\mathrm{R}}$ is exactly divergence-free and that the scheme is pressure-robust, i.e., the velocity does not change for other values of ν. The reduced schemes for $k = 2, 3, 4$ also produce optimally converging velocity and pressure approximations. Here the reduced scheme refers to the $\boldsymbol{P}_k - P_0$-like scheme in Subsection 6.2, while the full scheme refers to (3.2) with the enrichment space discussed in Subsection 2.3. For $k = 2$ the solutions of the full scheme and the reduced scheme coincide, while for $k > 2$ the solutions slightly differ in the sense that the $\boldsymbol{V}_h^{\mathrm{R}}$ is a bit larger in case of the reduced scheme.

7.2. **Example 2 - A three-dimensional example with analytic solutions.** On $\Omega = (0,1)^3$, the solution is prescribed as

$$\boldsymbol{u} = \frac{1}{2\pi}\operatorname{curl}\left\{[\sin(\pi x)\sin(\pi y)]^2 \sin(\pi z)\boldsymbol{e}_3\right\} \quad \text{and} \quad p = \sin(x)\sin(y)\sin(z) - (1-\cos 1)^3,$$

with $\boldsymbol{e}_3 = (0,0,1)^\top$. Again, we consider a Stokes equation with $\nu = 10^{-3}$ by choosing a suitable body force.

Figure 7.2 displays the convergence histories for the velocity and pressure errors, where the enrichment space discussed in Subsection 2.3 is employed. The expected convergence orders from Theorems 5.4 and 5.5 are obtained. The reduced scheme for $k = 2$ and $k = 3$ produces exactly the same solution as the full scheme, while solving a smaller linear system of equations.

8. Summary and outlook

This paper presents a novel way how to stabilize the Scott–Vogelius finite element method for arbitrary polynomial degree k and general shape-regular simplicial meshes that preserves optimal convergence and the divergence-free property of the velocity. This is realized by enriching the velocity space with carefully chosen Raviart–Thomas functions that stabilize the orthogonal complement of a small enough sub-pressure space that is known to be inf-sup stable. Finally, a reduced scheme is studied which only involves the degrees of freedom of the $\boldsymbol{H}^1$-conforming velocity and a piecewise constant pressure.

In the future, extensions to Navier–Stokes problems will be studied, which is able to preserve some conservation properties (e.g., conservation of linear momentum) and is *Re*-semi-robust. The latter property refers to estimates where the constants do not blow up as the Reynolds number becomes large.

References

[1] N. Ahmed, G. R. Barrenechea, E. Burman, J. Guzmán, A. Linke, and C. Merdon, *A pressure-robust discretization of Oseen's equation using stabilization in the vorticity equation*, SIAM J. Numer. Anal., 59 (2021), pp. 2746–2774.

[2] V. Anaya, A. Bouharguane, D. Mora, C. Reales, R. Ruiz-Baier, N. Seloula, and H. Torres, *Analysis and approximation of a vorticity-velocity-pressure formulation for the Oseen equations*, J. Sci. Comput., 80 (2019), pp. 1577–1606.

[3] D. N. Arnold, F. Brezzi, B. Cockburn, and L. D. Marini, *Unified analysis of discontinuous Galerkin methods for elliptic problems*, SIAM J. Numer. Anal., 39 (2002), pp. 1749–1779.

[4] D. N. Arnold and J. Qin, *Quadratic velocity/linear pressure Stokes elements*, Advances in Computer Methods for Partial Differential Equations-VII, R. Vichnevetsky, D. Knight & G. Richter, eds., IMACS, New Brunswick, NJ, (1992), pp. 28–34.

[5] L. Beirão da Veiga, F. Dassi, and G. Vacca, *Vorticity-stabilized virtual elements for the Oseen equation*, Math. Models Methods Appl. Sci., 31 (2021), pp. 3009–3052.

[6] C. Bernardi and G. Raugel, *Analysis of some finite elements for the Stokes problem*, Math. Comp., 44 (1985), pp. 71–79.

[7] D. Boffi, F. Brezzi, and M. Fortin, *Mixed finite element methods and applications*, vol. 44 of Springer Series in Computational Mathematics, Springer, Heidelberg, 2013.

[8] S. C. Brenner and L. R. Scott, *The mathematical theory of finite element methods*, vol. 15 of Texts in Applied Mathematics, Springer, New York, third ed., 2008.

[9] J. Carrero, B. Cockburn, and D. Schötzau, *Hybridized globally divergence-free LDG methods. I. The Stokes problem*, Math. Comp., 75 (2006), pp. 533–563.

[10] S. H. Christiansen and K. Hu, *Generalized finite element systems for smooth differential forms and Stokes' problem*, Numer. Math., 140 (2018), pp. 327–371.

[11] B. Cockburn, G. Kanschat, and D. Schötzau, *A note on discontinuous Galerkin divergence-free solutions of the Navier–Stokes equations*, J. Sci. Comput., 31 (2007), pp. 61–73.

[12] L. B. da Veiga, F. Dassi, D. A. D. Pietro, and J. Droniou, *Arbitrary-order pressure-robust DDR and VEM methods for the Stokes problem on polyhedral meshes*, arXiv, arXiv: 2112.09750 (2021).

[13] L. B. da Veiga, C. Lovadina, and G. Vacca, *Divergence free virtual elements for the Stokes problem on polygonal meshes*, ESAIM: M2AN, 51 (2017), pp. 509–535.

[14] J. de Frutos, B. Garcí a Archilla, V. John, and J. Novo, *Analysis of the grad-div stabilization for the time-dependent Navier–Stokes equations with inf-sup stable finite elements*, Adv. Comput. Math., 44 (2018), pp. 195–225.

[15] D. Frerichs and C. Merdon, *Divergence-preserving reconstructions on polygons and a really pressure-robust virtual element method for the Stokes problem*, IMA J. Numer. Anal., 42 (2022), pp. 597–619.

[16] B. García-Archilla, V. John, and J. Novo, *On the convergence order of the finite element error in the kinetic energy for high Reynolds number incompressible flows*, Comput. Methods Appl. Mech. Engrg., 385 (2021), pp. Paper No. 114032, 54.

[17] N. R. Gauger, A. Linke, and P. W. Schroeder, *On high-order pressure-robust space discretisations, their advantages for incompressible high Reynolds number generalised Beltrami flows and beyond*, SMAI J. Comput. Math., 5 (2019), pp. 89–129.

[18] V. Girault and P.-A. Raviart, *Finite element methods for Navier–Stokes equations*, vol. 5 of Springer Series in Computational Mathematics, Springer-Verlag, Berlin, 1986. Theory and algorithms.

[19] J. Guzmán and M. Neilan, *Conforming and divergence-free Stokes elements on general triangular meshes*, Math. Comp., 83 (2014), pp. 15–36.

[20] ———, *inf-sup stable finite elements on barycentric refinements producing divergence-free approximations in arbitrary dimensions*, SIAM J. Numer. Anal., 56 (2018), pp. 2826–2844.

[21] J. Guzmán and L. R. Scott, *Cubic Lagrange elements satisfying exact incompressibility*, SMAI J. Comput. Math., 4 (2018), pp. 345–374.

[22] J. Guzmán and L. R. Scott, *The Scott–Vogelius finite elements revisited*, Math. Comp., 88 (2019), pp. 515–529.

[23] Y. Han and Y. Hou, *Robust error analysis of H(div)-conforming DG method for the time-dependent incompressible Navier–Stokes equations*, J. Comput. Appl. Math., 390 (2021), pp. Paper No. 113365, 13.

[24] V. John, *Finite element methods for incompressible flow problems*, vol. 51 of Springer Series in Computational Mathematics, Springer, Cham, 2016.

[25] V. John, A. Linke, C. Merdon, M. Neilan, and L. G. Rebholz, *On the divergence constraint in mixed finite element methods for incompressible flows*, SIAM Rev., 59 (2017), pp. 492–544.

[26] P. L. Lederer, A. Linke, C. Merdon, and J. Schöberl, *Divergence-free reconstruction operators for pressure-robust Stokes discretizations with continuous pressure finite elements*, SIAM J. Numer. Anal., 55 (2017), pp. 1291–1314.

[27] C. Lehrenfeld, *Hybrid discontinuous Galerkin methods for incompressible flow problems*, master's thesis, RWTH Aachen, May 2010.

[28] C. Lehrenfeld and J. Schöberl, *High order exactly divergence-free hybrid discontinuous Galerkin methods for unsteady incompressible flows*, Comput. Methods Appl. Mech. Engrg., 307 (2016), pp. 339–361.

[29] X. Li and H. Rui, *A low-order divergence-free H(div)-conforming finite element method for Stokes flows*, IMA J. Numer. Anal, (2021). Published online.

[30] A. Linke and C. Merdon, *On velocity errors due to irrotational forces in the Navier–Stokes momentum balance*, J. Comput. Phys., 313 (2016), pp. 654–661.

[31] A. Linke and C. Merdon, *Pressure-robustness and discrete Helmholtz projectors in mixed finite element methods for the incompressible Navier–Stokes equations*, Comput. Methods Appl. Mech. Engrg., 311 (2016), pp. 304–326.

[32] A. Linke and L. G. Rebholz, *Pressure-induced locking in mixed methods for time-dependent Navier–Stokes equations*, J. Comput. Phys., 388 (2019), pp. 350–356.

[33] M. Neilan, *Discrete and conforming smooth de Rham complexes in three dimensions*, Math. Comp., 84 (2015), pp. 2059–2081.

[34] P. W. Schroeder, C. Lehrenfeld, A. Linke, and G. Lube, *Towards computable flows and robust estimates for inf-sup stable FEM applied to the time-dependent incompressible Navier–Stokes equations*, SeMA J., 75 (2018), pp. 629–653.

[35] P. W. Schroeder and G. Lube, *Pressure-robust analysis of divergence-free and conforming FEM for evolutionary incompressible Navier–Stokes flows*, J. Numer. Math., 25 (2017), pp. 249–276.
[36] L. R. Scott and M. Vogelius, *Conforming finite element methods for incompressible and nearly incompressible continua*, in Large-scale computations in fluid mechanics, Part 2 (La Jolla, Calif., 1983), vol. 22 of Lectures in Appl. Math., Amer. Math. Soc., Providence, RI, 1985, pp. 221–244.
[37] ———, *Norm estimates for a maximal right inverse of the divergence operator in spaces of piecewise polynomials*, ESAIM: Math. Model. Numer. Anal. - Modélisation Mathématique et Analyse Numérique, 19 (1985), pp. 111–143.
[38] J. Wang and X. Ye, *New finite element methods in computational fluid dynamics by H(div) elements*, SIAM J. Numer. Anal., 45 (2007), pp. 1269–1286.
[39] H. Wei, X. Huang, and A. Li, *Piecewise divergence-free nonconforming virtual elements for Stokes problem in any dimensions*, SIAM J. Numer. Anal., 59 (2021), pp. 1835–1856.
[40] S. Zaglmayr, *High Order Finite Element Methods for Electromagnetic Field Computation*, PhD thesis, Johannes Kepler University, August 2006.
[41] S. Zhang, *A new family of stable mixed finite elements for the 3D Stokes equations*, Math. Comp., 74 (2005), pp. 543–554.
[42] ———, *Divergence-free finite elements on tetrahedral grids for* $k \geqslant 6$, Math. Comp., 80 (2011), pp. 669–695.
[43] ———, *Quadratic divergence-free finite elements on Powell-Sabin tetrahedral grids*, Calcolo, 48 (2011), pp. 211–244.

Weierstrass Institute for Applied Analysis and Stochastics, Leibniz Institute in Forschungsverbund Berlin e.V. (WIAS), Mohrenstr. 39, 10117 Berlin, Germany and Freie Universität of Berlin, Department of Mathematics and Computer Science, Arnimallee 6, 14195 Berlin, Germany
Email address: john@wias-berlin.de

School of Mathematics, Shandong University, Jinan 250100, China
Email address: xulisdu@126.com

Weierstrass Institute for Applied Analysis and Stochastics, Leibniz Institute in Forschungsverbund Berlin e.V. (WIAS), Mohrenstr. 39, 10117 Berlin, Germany
Email address: merdon@wias-berlin.de

School of Mathematics, Shandong University, Jinan 250100, China
Email address: hxrui@sdu.edu.cn